

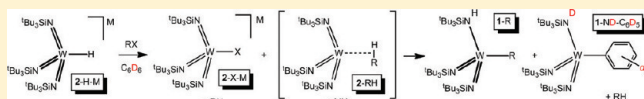
# Alkane Binding Implicated in Reactions of $(^t\text{Bu}_3\text{SiN}=\text{})_3\text{WHK}$ and Alkyl Halides

Daniel F. Schafer, II, Peter T. Wolczanski,\* and Emil B. Lobkovsky

Department of Chemistry & Chemical Biology, Baker Laboratory, Cornell University, Ithaca, New York 14853, United States

## Supporting Information

**ABSTRACT:** The reduction of alkyl, benzyl, allyl, and propargyl halides by  $[(^t\text{Bu}_3\text{SiN}=\text{})_3\text{WH}]\text{K}$  (**2-H-M**) was assayed via analysis of the product distributions. For unhindered  $\text{sp}^3$  substrates ( $\text{MeX}$ ,  $\text{EtX}$ ,  $\text{BnX}$ ,  $\text{CH}_2=\text{CHCH}_2\text{X}$ ,  $\text{RCCCH}_2\text{X}$ , etc.), the observed products were  $\text{RH}$  loss and  $[(^t\text{Bu}_3\text{SiN}=\text{})_3\text{WX}]\text{M}$  (**2-X-M**) or  $\text{MX}$  elimination and  $(^t\text{Bu}_3\text{SiNH})(^t\text{Bu}_3\text{SiN}=\text{})_2\text{WR}$  (**1-R**), which was derived from 1,2-RH-addition to an imide of the intermediate alkane (arene) complex  $(^t\text{Bu}_3\text{SiN}=\text{})_3\text{W}(\text{RH})$  (**2-RH**). Solvent activation or binding was also seen, consistent with the trapping of  $(^t\text{Bu}_3\text{SiN}=\text{})_3\text{W}$  (**2**) generated from  $\text{RH}$  loss from **2-RH**. The radical clocks  $^i\text{PrCH}_2\text{Br}$  and 5-hexenyl bromide yielded the unrearranged products  $(^t\text{Bu}_3\text{SiNH})(^t\text{Bu}_3\text{SiN}=\text{})_2\text{W}(\text{trans-}^i\text{C}(\text{CHCH}_2\text{CHMe}))$  (**1- $^i\text{PrMe}$** ) and  $(^t\text{Bu}_3\text{SiNH})(^t\text{Bu}_3\text{SiN}=\text{})_2\text{W}(\text{trans-CH=CH}^n\text{Bu})$  (**1-CH=CH $^n$ Bu**), respectively. When hindered  $\text{sp}^3$  substrates were employed, halogenated products  $[(^t\text{Bu}_3\text{SiN}=\text{})_3\text{WX}]\text{M}$  (**2-X-M**) and  $(^t\text{Bu}_3\text{SiNH})(^t\text{Bu}_3\text{SiN}=\text{})_2\text{WX}$  (**1-X**) were prominent, suggesting that radical paths were operable. KIEs derived from product ratios involving  $\text{CD}_3\text{I}$  or  $\text{CD}_3\text{CH}_2\text{I}$  and **2-H-K** supported the intermediacies of  $(^t\text{Bu}_3\text{SiN}=\text{})_3\text{W}(\text{CHD}_3)$  (**2-CHD $_3$** ) and  $(^t\text{Bu}_3\text{SiN}=\text{})_3\text{W}(\text{CH}_3\text{CD}_3)$  (**2-CH $_3$ CD $_3$** ), respectively. X-ray crystal structures of  $(^t\text{Bu}_3\text{SiNH})(^t\text{Bu}_3\text{SiN}=\text{})_2\text{WR}$  (**1-R**;  $\text{R} = \text{Me}$ ,  $^i\text{PrMe}$ ,  $\text{CH}=\text{C}=\text{CH}_2$ ) are presented, and the results are placed in the context of 1,2-RH-addition to  $\text{d}^0$  early-transition-metal imido species.



## INTRODUCTION

Evidence for the intermediacy of alkane complexes in reactions that ultimately cleave carbon–hydrogen bonds is compelling in several  $\text{d}^6$  and  $\text{d}^8$  systems. The direct observation of a methane complex of rhodium,  $[\{2,6-(^t\text{Bu}_2\text{PO})\text{C}_5\text{H}_4\text{N}\}\text{Rh}(\text{CH}_4)]\text{BAR}^{\text{F}}_4$ ,<sup>1</sup> is a recent highlight that followed related low-temperature NMR spectroscopic characterizations of cyclopentane<sup>2</sup> and cyclohexane<sup>3</sup> adducts of rhenium, i.e.,  $\text{CpRe}(\text{CO})_2(\text{AlkH})$ , among others.<sup>4–6</sup> Previously, indirect characterizations of  $\text{M}(\text{RH})$  species by dynamic NMR spectroscopy were implicated in the interconversion of hydride and methyl resonances in tungsten,<sup>7</sup> rhenium,<sup>8</sup> osmium,<sup>9</sup> and iridium<sup>10</sup> complexes and via chain-walking in  $\text{Cp}^*\text{Rh}(\text{PMe}_3)\text{R}(\text{H})$  species,<sup>11</sup> where the alkane adduct was a logical intermediate in oxidative addition/reductive elimination events. While not precursors to oxidative addition, a heptane bound within a porphyrin pocket<sup>12</sup> and several cyclic alkanes embedded within the arms of a tacn ligand, i.e.,  $[\kappa\text{-O}_3\text{N}_3\text{-(2,4-(^t\text{Bu})C}_6\text{H}_2\text{O(6-CH}_2\text{)}_2\text{tacn)]U}(\text{RH})$ ,<sup>13</sup> have been crystallographically characterized.

In  $\text{d}^0$  carbon–hydrogen bond activation systems where 1,2-RH-addition to a metal–imido linkage of  $\text{XYM}=\text{NR}$  constitutes the activation event,<sup>14</sup> the intermediacy of alkane complexes was implicated by calculations<sup>15–18</sup> but unobserved by spectroscopy. Observations of 1,2-RH elimination from  $\text{XY}(\text{R}'\text{NH})\text{M}-\text{R}$  and corresponding calculations were in concert in suggesting that dynamic exchange of the amide hydrogen with hydrogens on the alkyl was energetically unfeasible. Competitive loss of  $\text{RH}$  was too swift with respect to alkane readdition in  $(^t\text{Bu}_3\text{SiO})_2(^t\text{Bu}_3\text{SiNH})\text{TiR}$ ,<sup>19–21</sup>

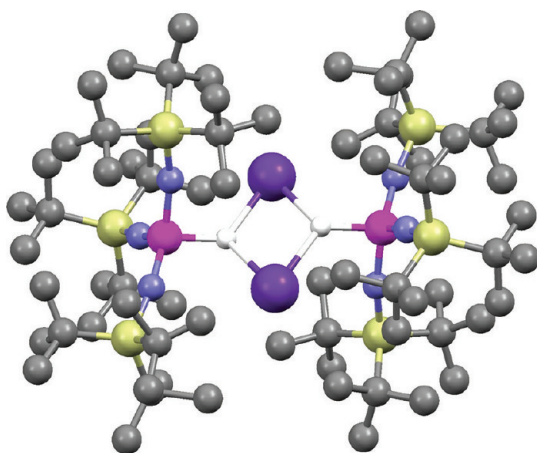
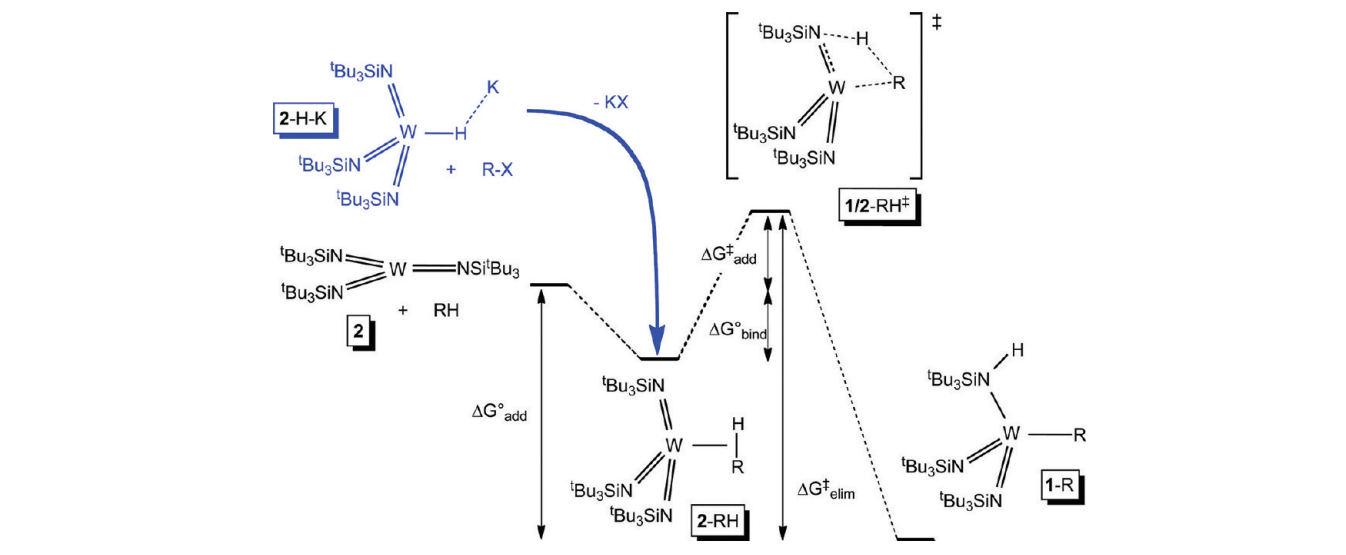
$(^t\text{Bu}_3\text{SiNH})_3\text{TiR}$ ,<sup>22</sup>  $(^t\text{Bu}_3\text{SiNH})_3\text{ZrR}$ ,<sup>23,24</sup>  $(^t\text{Bu}_3\text{SiNH})_2(^t\text{Bu}_3\text{SiN}=\text{})\text{VR}$ ,<sup>25,26</sup> and  $(^t\text{Bu}_3\text{SiNH})_2(^t\text{Bu}_3\text{SiN}=\text{})\text{TaR}$ <sup>27</sup> systems. Moreover, for related tungsten imido complexes, 1,2-RH-elimination from  $(^t\text{Bu}_3\text{SiNH})(^t\text{Bu}_3\text{SiN}=\text{})_2\text{WR}$  (**1-R**) was not observed (Scheme 1). As previously shown, extended thermolysis of  $(^t\text{Bu}_3\text{SiNH})(^t\text{Bu}_3\text{SiN}=\text{})_2\text{WCD}_3$  (**1-CD $_3$** ) in  $\text{C}_6\text{H}_6$  at 200 °C revealed no H/D exchange between amide and methyl positions, nor was any solvent activation indicated, consistent with calculations on  $(\text{NH}_2)(\text{HN}=\text{})_2\text{WCH}_3$  that suggested  $\Delta H^\ddagger_{\text{elim}}$  was  $\sim 60$  kcal/mol.<sup>28–30</sup>

While the activation energy pertaining to 1,2-elimination of  $\text{MeH}$  from  $(^t\text{Bu}_3\text{SiNH})(^t\text{Bu}_3\text{SiN}=\text{})_2\text{WCH}_3$  (**1-CH $_3$** )—or the corresponding calculated elimination from  $(\text{NH}_2)(\text{HN}=\text{})_2\text{WCH}_3$ —appeared prohibitive with regard to the observation of a methane adduct, its binding energy was expected to be substantial on the basis of a calculated  $\Delta G^\circ_{\text{bind}}$  value of  $-8.4$  kcal/mol ( $\Delta H^\circ_{\text{bind}} \approx -15.6$  kcal/mol) for  $(\text{HN}=\text{})_3\text{W}(\text{CH}_4)$ .<sup>17,18</sup> A significant experimental break occurred when anionic hydride adducts of  $(^t\text{Bu}_3\text{SiN}=\text{})_3\text{W}$  (**2**) were synthesized via the methodology previously delineated.<sup>28–30</sup> While  $[(^t\text{Bu}_3\text{SiN}=\text{})_3\text{WH}]\text{K}$  (**2-H-K**) possesses the solubility properties of a monomer, Figure 1 illustrates its solid-state structure, which is a  $\text{C}_{2h}$ -symmetric dimer containing potassiums bridging anionic  $[(^t\text{Bu}_3\text{SiN}=\text{})_3\text{WH}]^-$  units.<sup>29,30</sup> As Scheme 1 illustrates, the treatment of **2-H-K** with alkyl halides provided hints of alkane

Received: October 5, 2011

Published: November 29, 2011

Scheme 1



**Figure 1.** Ball and stick view of the solid-state dimer of 2-H-K: i.e.,  $[(^t\text{Bu}_3\text{SiN}=\text{W})_3\text{WH}]_2(\mu\text{-K})_2$  ( $(2-\text{H})_2(\mu\text{-K})_2$ ).

complex intermediates, as the transfer of hydride from 2-H-K to  $\text{RX}$  provided a separate, indirect path to these transient species. In essence, the results implied that the free energy well in which  $(^t\text{Bu}_3\text{SiN}=\text{W})(\text{RH})$  (2-RH) existed was deep enough that  $\text{CH}$  activation to give  $(^t\text{Bu}_3\text{SiNH})(^t\text{Bu}_3\text{SiN}=\text{W})\text{R}$  (1-R) could be competitive with alkane loss in certain instances. Detailed investigations into the probable intermediacy of alkane complexes are delineated below; a portion of this effort has been communicated.<sup>28</sup>

## RESULTS

**$[(^t\text{Bu}_3\text{SiN}=\text{W})_3\text{WH}]\text{K}$  (2-H-K) and  $\text{RX}$ .** As a hydride source,  $[(^t\text{Bu}_3\text{SiN}=\text{W})_3\text{WH}]\text{K}$  (2-H-K) proved most convenient to synthesize, and it was used almost exclusively in these investigations. Reactions were typically run with  $\text{RX}$  in excess, i.e., pseudo-first-order conditions, for reasonable conversions. Many of the products, such as  $(^t\text{Bu}_3\text{SiNH})(^t\text{Bu}_3\text{SiN}=\text{W})\text{R}$  (1-R),  $(^t\text{Bu}_3\text{SiNH})(^t\text{Bu}_3\text{SiN}=\text{W})\text{X}$  (1-X), and  $[(^t\text{Bu}_3\text{SiN}=\text{W})_3\text{WX}]\text{K}$  (2-X-K), have been previously synthesized and characterized;<sup>30</sup> NMR spectroscopic data for any new compounds are given in Table 1.

**$[(^t\text{Bu}_3\text{SiN}=\text{W})_3\text{WH}]\text{M}$  (2-H-M) and  $\text{MeX}$ .** 1. *Product Distributions.* As previously reported,<sup>30</sup> treatment of

$[(^t\text{Bu}_3\text{SiN}=\text{W})_3\text{WH}]\text{K}$  (2-H-K) with  $\text{MeI}$  in  $\text{THF-}d_8$  generated  $\sim 12\%$  of  $(^t\text{Bu}_3\text{SiNH})(^t\text{Bu}_3\text{SiN}=\text{W})\text{CH}_3$  (1-CH<sub>3</sub>), a result made consistent with a methane complex intermediate. A switch to benzene as solvent rendered this possibility more tenable, as heating 2-H-K with 10 equiv of  $\text{CH}_3\text{I}$  in  $\text{C}_6\text{D}_6$  at  $60^\circ\text{C}$  for 6 h produced 1-CH<sub>3</sub> in 90% yield by  $^1\text{H}$  NMR spectroscopy, accompanied by 10%  $(^t\text{Bu}_3\text{SiND})(^t\text{Bu}_3\text{SiN}=\text{W})\text{WC}_6\text{D}_5$  (1-ND- $\text{C}_6\text{D}_5$ ), representing activation of the solvent, trace amounts of  $[(^t\text{Bu}_3\text{SiN}=\text{W})_3\text{WI}]\text{K}$  (2-I-K,  $<2\%$ ) and  $\text{CH}_4$ , and a precipitate, presumed to be  $\text{KI}$  (Scheme 2). Use of  $\text{CD}_3\text{I}$  as the substrate (10 equiv) afforded  $\sim 70\%$  1- $\text{CD}_3$  and  $(^t\text{Bu}_3\text{SiND})(^t\text{Bu}_3\text{SiN}=\text{W})\text{WCD}_2\text{H}$  (1-ND- $\text{CD}_2\text{H}$ ), an increased amount of 1-ND- $\text{C}_6\text{D}_5$  (22%), and a measurable amount ( $\sim 8\%$ ) of  $[(^t\text{Bu}_3\text{SiN}=\text{W})_3\text{WI}]\text{K}$  (2-I-K) along with trace  $\text{CD}_3\text{H}$ . It proved difficult to obtain the ratio 1- $\text{CD}_3$ /1-ND- $\text{CD}_2\text{H}$  by  $^1\text{H}$  NMR spectroscopy due to problems assessing the magnitude of the  $-\text{CD}_2\text{H}$  quintet at the foot of a much larger resonance. A decline in the integrated NH resonance relative to the 54 H imide methyl resonance from  $0.86(2)/54$  vs  $1.02(2)/54$  in samples of 1-CH<sub>3</sub> was consistent with the formation of some 1-ND- $\text{CD}_2\text{H}$ . To check for the possibility of exogenous methane activation, the experiment was repeated with 5 equiv of  $\text{CH}_4$  present, and only  $\text{CD}_3\text{H}$ -derived products were generated ( $\sim 65\%$ ) along with 9% of 2-I-K. Little if any 1-CH<sub>3</sub> was detected ( $<5\%$ ), consistent with methane activation solely from  $\text{CD}_3\text{H}$ . The potassium iodide adduct 2-I-K is *not* the origin of methane or benzene solvent activation, as independent thermolyses confirmed its stability. What is not clear is whether solvent activation occurs during the alkylation process or whether it is due to the capture of putative  $(^t\text{Bu}_3\text{SiN}=\text{W})_3\text{W}$  (2) formed via  $\text{MeH}$  escape from 2-MeH.

The ratio 1- $\text{CD}_3$ /1-ND- $\text{CD}_2\text{H}$  was determined from a separate experiment conducted in  $\text{C}_6\text{H}_6$ , so that  $^2\text{H}\{^1\text{H}\}$  NMR could be used for the assay. Under the same conditions, 73% 1- $\text{CD}_3$  and 1-ND- $\text{CD}_2\text{H}$  were obtained, with 27%  $(^t\text{Bu}_3\text{SiNH})(^t\text{Bu}_3\text{SiN}=\text{W})\text{Ph}$  (1-Ph) and  $<2\%$  2-I-K. The relative integrated intensity of the methyl resonance at  $\delta$  1.41 to the amide at  $\delta$  6.60 was 11.5(8). Assuming the only two contributing molecules to these resonances are 1- $\text{CD}_3$  and 1-ND- $\text{CD}_2\text{H}$ , the ratio 1- $\text{CD}_3$ /1-ND- $\text{CD}_2\text{H}$  was 3.2(2)/1, and after multiplying by the statistical factor of 3, the  $k_{\text{H}}/k_{\text{D}}$  value for intramolecular methane activation via putative

Table 1.  $^1\text{H}$  and  $^{13}\text{C}\{^1\text{H}\}$  NMR Spectral Assignments<sup>a</sup> for  $(^t\text{Bu}_3\text{SiNH})(^t\text{Bu}_3\text{SiN}=\text{})_2\text{WX/R}$  (1-X/R) and  $(^t\text{Bu}_3\text{SiN}=\text{})_3\text{WL}$ 

compd	$^1\text{H}$ NMR ( $\delta$ (mult, $J$ (Hz), assignt))		$^{13}\text{C}\{^1\text{H}\}$ NMR ( $\delta$ ( $J$ (Hz), assignt))		
	$^t\text{Bu}^b$	NH and R	$\text{SiCMe}_3^b$	$\text{SiC}(\text{CH}_3)_3^b$	R
$(^t\text{Bu}_3\text{SiN}=\text{})_3\text{WOEt}_2$ (2-OEt <sub>2</sub> )	1.40	0.70 (t, 7, CH <sub>3</sub> ) 4.09 (q, 7, CH <sub>2</sub> )	24.40	31.55	12.80 (CH <sub>3</sub> ) 80.29 (CH <sub>2</sub> )
$(^t\text{Bu}_3\text{SiN}=\text{})_3\text{W}(\text{THF})$ (2-THF)	1.42	0.96 (m, CH <sub>2</sub> ) 4.16 (m, OCH <sub>2</sub> )	24.33	31.54	26.01 (CH <sub>2</sub> ) 85.91 (OCH <sub>2</sub> )
$(^t\text{Bu}_3\text{SiN}=\text{})_2(^t\text{Bu}_3\text{SiNH})\text{W}^c\text{PrMe}$ (1- <sup>c</sup> PrMe) <sup>c,d</sup>	1.24	6.30 (NH)	23.44	30.79	21.92 (C <sup>4</sup> H <sub>3</sub> )
	1.35	1.06 (3.5 <sup>3c3t</sup> , 5.1 <sup>23t</sup> , 9.2 <sup>13t</sup> , C <sup>3</sup> H <sup>1</sup> )	24.40	31.22	21.92 (C <sup>2</sup> H)
		1.14 (5.9 <sup>24</sup> , C <sup>4</sup> H <sub>3</sub> )			22.97 (C <sup>3</sup> H)
		1.65 (5.3 <sup>12</sup> , 6.5 <sup>13c</sup> , 9.2 <sup>13t</sup> , C <sup>1</sup> H)			49.48 ( <sup>1</sup> J <sub>WC</sub> = 187, C <sup>1</sup> H)
		1.89 (3.5 <sup>3c3t</sup> , 6.5 <sup>13c</sup> , 7.1 <sup>23c</sup> , C <sup>3</sup> H <sup>c</sup> ) 2.09 (5.1 <sup>23t</sup> , 5.3 <sup>12</sup> , 5.9 <sup>24</sup> , 7.1 <sup>23c</sup> , C <sup>2</sup> H)			
$(^t\text{Bu}_3\text{SiN}=\text{})_2(^t\text{Bu}_3\text{SiNH})\text{W}(\text{CH}=\text{CEt})$ (1-CH=CH <sup>e</sup> Et)	<i>e</i>	6.76 (NH)  6.94 (dt, 17, 6.5, CH <sup>e</sup> Et) 7.90 (d, 17, WCH)			
$(^t\text{Bu}_3\text{SiN}=\text{})_2(^t\text{Bu}_3\text{SiNH})\text{W}(\text{CH}=\text{C}^n\text{Bu})$ (1-CH=CH <sup>n</sup> Bu) <sup>f</sup>	1.24	6.62 (NH)	23.57	30.80	22.37 (CH <sub>3</sub> )
	1.36	0.84 (t, 7, CH <sub>3</sub> ) 2.06 (m, CHCH <sub>2</sub> ) 8.01 (d, 17, WCH)	24.54	31.26	24.95 (CH <sub>2</sub> ) 31.89 (CH <sub>2</sub> ) 38.50 (CH <sub>2</sub> ) 158.90 (CH) 166.19 (CH)
$(^t\text{Bu}_3\text{SiNH})(^t\text{Bu}_3\text{SiN}=\text{})_2\text{W}(\text{CH}_2\text{C}_6\text{H}_4\text{-}p\text{-Me})$ (1-xyl)	1.22	6.71 (NH)	23.38	30.81	<i>g</i>
	1.29	2.20 (CH <sub>3</sub> ) 3.59 ( <i>J</i> <sub>WH</sub> = 15, CH <sub>2</sub> ) 7.01 (d, 7, CH) 7.24 (d, 7, CH)			
$(^t\text{Bu}_3\text{SiNH})(^t\text{Bu}_3\text{SiN}=\text{})_2\text{W}(\text{C}_6\text{H}_3\text{-}2,5\text{-Me}_2)$ (1-2,5-Me <sub>2</sub> Ph) <sup>h</sup>	1.21	6.83 (NH)	23.53	30.93	20.21 (CH <sub>3</sub> )
	1.37	2.21 (CH <sub>3</sub> ) 2.85 (CH <sub>3</sub> ) 6.90 (d, 8, CH) 8.71 (s, CH)	24.70	31.51	24.49 (CH <sub>3</sub> ) 129.42 (Ar) 130.75 (Ar) 133.17 (Ar) 142.62 (Ar) 148.08 (C <sub>ipso</sub> )
					21.63 (CH <sub>3</sub> )
$(^t\text{Bu}_3\text{SiNH})(^t\text{Bu}_3\text{SiN}=\text{})_2\text{W}(2\text{-C}_{10}\text{H}_6\text{-}6\text{-Me})(1\text{-}6\text{-Me-}2\text{-nap})^i$	1.21	6.95 (NH)	23.57	30.80	
	1.40	2.16 (CH <sub>3</sub> ) 7.09 (d, 8, CH) 7.28 (CH <sup>5</sup> ) 7.61 (d, 8, CH) 7.78 (d, 8, CH) 8.50 (d, 8, CH) 9.15 (CH <sup>1</sup> )	24.59	31.33	125.73 (Ar) 127.37 (Ar) 128.49 (Ar) 132.29 (Ar) 134.15 (Ar) 136.46 (Ar) 139.18 (Ar) 144.95 (Ar) 171.97 (C <sub>ipso</sub> )
					21.63 (CH <sub>3</sub> )
$(^t\text{Bu}_3\text{SiNH})(^t\text{Bu}_3\text{SiN}=\text{})_2\text{W}(2\text{-C}_{10}\text{H}_6\text{-}7\text{-Me})(1\text{-}7\text{-Me-}2\text{-nap})^i$	1.21	6.97 (NH)	23.57	30.80	
	1.40	2.18 (CH <sub>3</sub> ) 7.02 (d, 8, CH) 7.46 (d, 8, CH) 7.61 (d, 8, CH) 7.69 (CH <sup>8</sup> ) 8.46 (d, 8, CH) 9.13 (CH <sup>1</sup> )	24.59	30.80	126.09 (Ar) 127.15 (Ar) 129.10 (Ar) 132.20 (Ar) 134.26 (Ar) 135.78 (Ar) 138.35 (Ar) 144.37 (Ar) 172.90 (C <sub>ipso</sub> )

Table 1. continued

compd	<sup>1</sup> H NMR (δ (mult, J (Hz), assign))		<sup>13</sup> C{ <sup>1</sup> H} NMR (δ (J (Hz), assign))		
	<sup>t</sup> Bu <sup>b</sup>	NH and R	SiCMe <sub>3</sub> <sup>b</sup>	SiC(CH <sub>3</sub> ) <sub>3</sub> <sup>b</sup>	R
(tBu <sub>3</sub> SiNH)(tBu <sub>3</sub> SiN=)W(CH <sub>2</sub> C <sub>6</sub> H <sub>3</sub> -3,5-Me <sub>2</sub> ) (1-mes)	1.23	6.71 (NH)	23.39	30.83	21.38 (CH <sub>3</sub> )
	1.29	2.19 (CH <sub>3</sub> )	24.49	31.14	50.92 (CH <sub>2</sub> )
		3.58 (J <sub>WH</sub> = 15, CH <sub>2</sub> )			126.62 (Ar)
		6.55 (CH <sup>d</sup> )			127.66 (Ar)
		6.98 (CH <sup>2,6</sup> )			137.54 (Ar)
(tBu <sub>3</sub> SiNH)(tBu <sub>3</sub> SiN=)W(CH=C=CH <sub>2</sub> ) (1-CH=C=CH <sub>2</sub> )	1.22	6.87 (NH)	23.53	30.76	67.08 ( <sup>3</sup> J <sub>WC</sub> = 7, CH <sub>2</sub> )
	1.33	4.35 (d, 7, <sup>4</sup> J <sub>WH</sub> = 7, CH <sub>2</sub> )	24.54	31.24	109.08 ( <sup>1</sup> J <sub>WC</sub> = 179, CH)
		6.70 (t, 7, <sup>2</sup> J <sub>WH</sub> = 7, CH)			212.07 (C)
(tBu <sub>3</sub> SiNH)(tBu <sub>3</sub> SiN=)WSiMe <sub>3</sub> (1-SiMe <sub>3</sub> )	1.19	6.97 (NH)	23.10	30.64	10.08 (CH <sub>3</sub> )
	1.34	0.81 (CH <sub>3</sub> )	24.13	31.24	
(tBu <sub>3</sub> SiN=) <sup>k</sup> W(κ-C,N,C-N(Si <sup>t</sup> Bu <sub>3</sub> )CHC(Me)-) (3-HCCMe)	1.17 <sup>j</sup>	2.62 (d, 2, <sup>3</sup> J <sub>WH</sub> = 13, CH <sub>3</sub> )	23.52 <sup>j</sup>	30.89 <sup>j</sup>	
	1.32	5.89 (q, 2, <sup>3</sup> J <sub>WH</sub> = 54, CH)	24.23	31.06	
(tBu <sub>3</sub> SiN=) <sub>2</sub> W(κ-C,N,C-N(Si <sup>t</sup> Bu <sub>3</sub> )CMeCMe-) (3-MeCCMe)	1.22 <sup>j</sup>	2.28 (CH <sub>3</sub> )	24.8 <sup>l</sup>	31.26 <sup>l</sup>	15.81 ( <sup>3</sup> J <sub>WC</sub> = 26, CH <sub>3</sub> )
	1.32	2.52 ( <sup>3</sup> J <sub>WH</sub> = 13, CH <sub>3</sub> )	24.32	31.13	20.71 ( <sup>4</sup> J <sub>WC</sub> = 9, CH <sub>3</sub> )
					126.23 ( <sup>2</sup> J <sub>WC</sub> = 15, WCC)
(tBu <sub>3</sub> SiN=) <sub>2</sub> W(κ-C,η <sup>3</sup> -C,N-CH <sub>2</sub> CMe <sub>2</sub> Si( <sup>t</sup> Bu <sub>2</sub> )NCMeCHMe) (4-MeCCMe)	1.27	1.04 (Si <sup>t</sup> Bu)	21.30	31.20	16.66 (C(CH <sub>3</sub> )Me)
	1.37	1.21 (Si <sup>t</sup> Bu)	24.64	31.36	22.91 (CMe(CH <sub>3</sub> ))
	1.48	C(CH <sub>3</sub> )Me			23.41 (SiC)
	1.50	CMe(CH <sub>3</sub> )			24.46 (SiC)
	1.82	(d, 5.5, NCCCH <sub>3</sub> )			33.54 (NCCCH <sub>3</sub> )
	2.31	(NCCCH <sub>3</sub> )			33.79 (NCCCH <sub>3</sub> )
	2.60	(d, 13, <sup>2</sup> J <sub>WH</sub> = 10, WCHH)			35.29 (CH <sub>2</sub> CMe <sub>2</sub> )
	2.75	(d, 13, <sup>2</sup> J <sub>WH</sub> = 10, WCHH)			53.28 (J <sub>WC</sub> = 24, NCC)
	3.18	(q, 5.5, NCCH)			54.08 ( <sup>1</sup> J <sub>WC</sub> = 105, WCH <sub>2</sub> )
					180.47 ( <sup>2</sup> J <sub>WC</sub> = 10, NC)

<sup>a</sup>In benzene-*d*<sub>6</sub> unless otherwise noted. All *J*<sub>WH</sub> values reported were obtained from W satellites that integrated to ~14% intensity, indicative of one tungsten center. <sup>b</sup>The amide is listed first and the imide second. <sup>c</sup>From E.COSY and HMQC experiments: W-<sup>c</sup>(C<sup>1</sup>HC<sup>2</sup>H(C<sup>4</sup>H<sub>3</sub>)C<sup>3</sup>H<sup>4</sup>H<sup>t</sup>), e.g., <sup>3</sup>J<sub>13t</sub> = 9.2 Hz listed as 9.2<sup>13t</sup>. <sup>d1</sup>J<sub>CH</sub> = 145 (C<sup>1</sup>H), 163 (C<sup>2</sup>H), 161 (C<sup>3</sup>H<sup>4</sup>), 160 (C<sup>4</sup>H<sup>t</sup>), 126 Hz (C<sup>4</sup>H<sub>3</sub>). <sup>e</sup>Resonances obscured by the major product 1-<sup>c</sup>PrMe. <sup>f</sup>Methylene obscured by the <sup>t</sup>Bu<sub>3</sub> group and CH obscured by the residual solvent in <sup>1</sup>H NMR. <sup>g</sup>Minor product (14%); hence, aryl carbons are not observed. <sup>h</sup>Aryl resonance obscured by residual solvent; one CMe not observed. <sup>i</sup>One aryl carbon not observed; assignments tentative due to overlapping resonances, and similar intensities with isomer. <sup>j</sup>Metallacyclic NSi<sup>t</sup>Bu<sub>3</sub> listed first. <sup>k</sup>Since the metallacycle is a minor product, carbon resonances are not identified with confidence. <sup>l</sup>Metallacyclic NSi<sup>t</sup>Bu<sub>3</sub> resonances listed first; both are broad.

(tBu<sub>3</sub>SiN=)<sub>3</sub>W(CD<sub>3</sub>H) (2-CD<sub>3</sub>H) was 9.6(6). As previously stated, the isotopomers do not thermally interconvert; hence, the ratio reflects a kinetic product distribution. Herein it is also assumed that differential binding of the methane, e.g., (tBu<sub>3</sub>SiN=)<sub>3</sub>W(η<sup>2</sup>-HD<sub>2</sub>CD<sub>2</sub>) vs (tBu<sub>3</sub>SiN=)<sub>3</sub>W(η<sup>2</sup>-D<sub>2</sub>CHD), is fast and reversible; hence, the KIE reflects the relative transition states for CH vs CD activation. Nonetheless, the KIE must be considered a phenomenological number reflecting both binding and activation events.

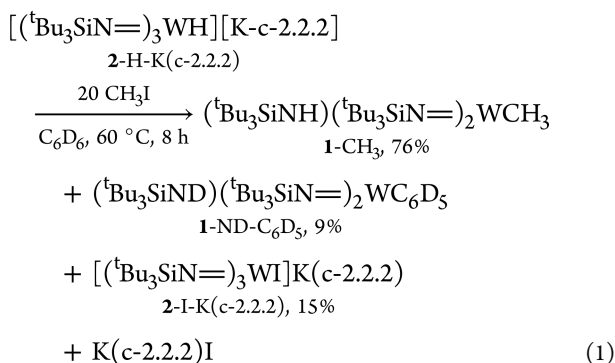
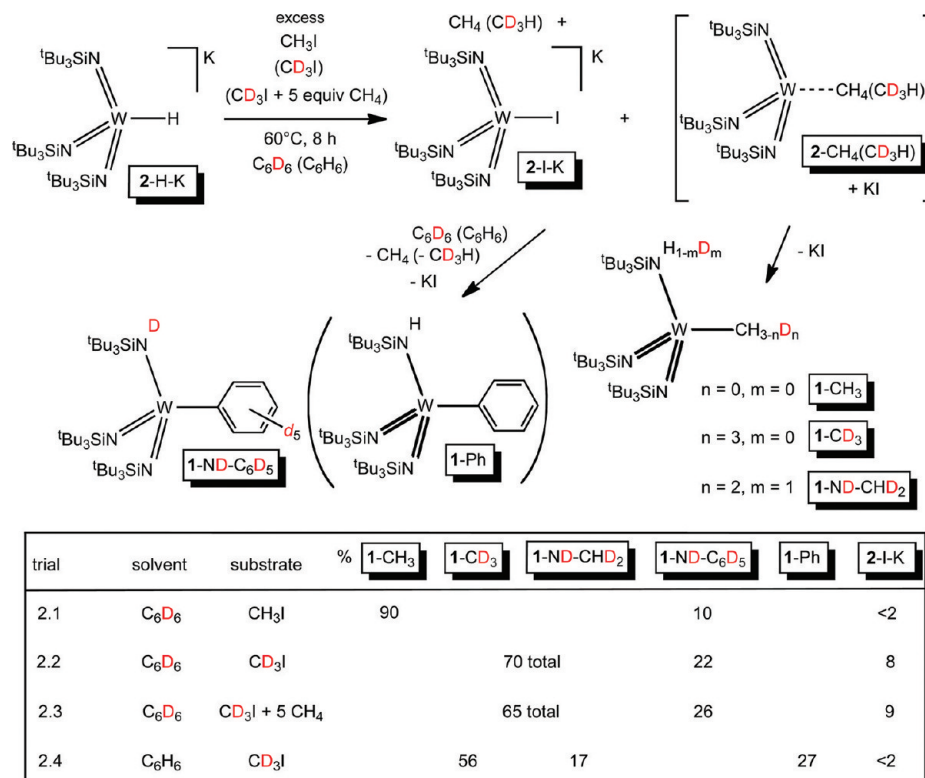
The potassium counterion may or may not be bound to the [(tBu<sub>3</sub>SiN=)<sub>3</sub>WH] core in 2-H-K during the course of methyl halide addition; therefore, [(tBu<sub>3</sub>SiN=)<sub>3</sub>WH][K-c-2.2.2] (2-

H-K(c-2.2.2)),<sup>30</sup> where the K<sup>+</sup> is complexed by crypt-2.2.2, was used in a CH<sub>3</sub>I reaction according to eq 1. The results are quite similar to the previous trials, with the 76% conversion to (tBu<sub>3</sub>SiNH)(tBu<sub>3</sub>SiN=)<sub>2</sub>WCH<sub>3</sub> (1-CH<sub>3</sub>) comparable to trial 2.1 in Scheme 2. No evidence of uncomplexed crypt-2.2.2 was obtained by <sup>1</sup>H NMR spectroscopic analysis, and the observed crypt-2.2.2 was attributable to 15% [(tBu<sub>3</sub>SiN=)<sub>3</sub>WI]K(c-2.2.2) (2-I-K(c-2.2.2)).

A switch to donor solvents (Scheme 3) for the addition of CD<sub>3</sub>I to [(tBu<sub>3</sub>SiN=)<sub>3</sub>WH]K (2-H-K) did not change the amount of methane activation under comparable conditions (60 °C, 10 h), as 73% (tBu<sub>3</sub>SiNH)(tBu<sub>3</sub>SiN=)<sub>2</sub>WCD<sub>3</sub> (1-



Scheme 2



CD<sub>3</sub>) and (tBu<sub>3</sub>SiND)(tBu<sub>3</sub>SiN)<sub>2</sub>WCD<sub>2</sub>H (1-ND-CD<sub>2</sub>H) formed in diethyl ether. Instead of solvent activation, binding of Et<sub>2</sub>O was noted in the form of (tBu<sub>3</sub>SiN)<sub>3</sub>W(OEt<sub>2</sub>) (2-OEt<sub>2</sub>, 27%), and no 2-K-I was observed. At a higher temperature (100 °C, 75 min), a similar reaction in THF afforded only 33% methane activation, and the major product was the THF adduct (tBu<sub>3</sub>SiN)<sub>3</sub>W(THF) (2-THF, 45%), accompanied by 22% 2-I-K. The deuterium incorporation in the amide position was assayed by <sup>2</sup>H{<sup>1</sup>H} NMR spectroscopy to provide *k<sub>H</sub>*/*k<sub>D</sub>* values for HCD<sub>3</sub> activation of 9.9(6) in Et<sub>2</sub>O and 11.7(6) in THF.

Some modest hydride and substrate variations were tested in C<sub>6</sub>D<sub>6</sub>, and the results are given in Scheme 4. One assumption is with regard to the structure of [(tBu<sub>3</sub>SiN)<sub>3</sub>WH]Na (2-H-Na), which is presumed to be similar to that of 2-H-K. At 60 °C, it appears that the nature of CH<sub>3</sub>X (X = Cl, Br, I) has little effect on the product distribution, with 88–90% (tBu<sub>3</sub>SiNH)-(tBu<sub>3</sub>SiN)<sub>2</sub>WCH<sub>3</sub> (1-CH<sub>3</sub>), 8–10% (tBu<sub>3</sub>SiND)(tBu<sub>3</sub>SiN)<sub>2</sub>WC<sub>6</sub>D<sub>5</sub> (1-ND-C<sub>6</sub>D<sub>5</sub>), and very little 2-X-K (≤3%) produced. At lower temperature (23 °C), a greater amount (~32%) of 2-X-K is generated while the 1-CH<sub>3</sub>/1-ND-C<sub>6</sub>D<sub>5</sub>

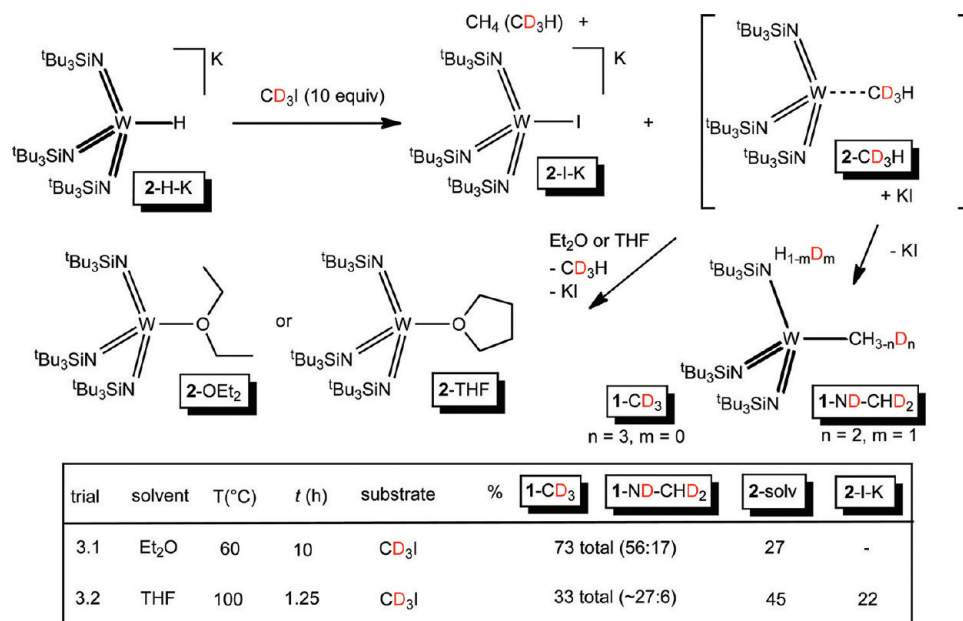
(~68% total) ratio remains essentially the same for both X = Br and X = I. Use of 2-H-Na (trial 4.2) causes a significant increase in 2-I-Na vs 2-I-K production in trial 4.1, although the 1-CH<sub>3</sub>/1-ND-C<sub>6</sub>D<sub>5</sub> ratio is similar.

Nucleophilic and electron transfer mechanisms for CH<sub>3</sub>X reduction should depend on the nature of X, but if the transition state for this component of the overall process is very early, it is possible that the product distribution would not be very sensitive to these changes. Note that the methane vs solvent activation ratio is relatively constant for all trials, perhaps indicating that the latter is derived from dissociation of CH<sub>4</sub> from putative transient (tBu<sub>3</sub>SiN)<sub>3</sub>W(CH<sub>4</sub>) (2-CH<sub>4</sub>). It is also plausible that the Na counterion has a greater affinity for heteroatoms in the core of the tungsten hydride; hence, collapse to the NaI adduct in trial 4.2 is more favorable than in the related reaction with potassium (trial 4.1). In the reaction of CH<sub>3</sub>I with 2-H-Na, a small amount (4%) of (tBu<sub>3</sub>SiNH)-(tBu<sub>3</sub>SiN)<sub>2</sub>WI (1-I) is also produced, but its origin is not clear.

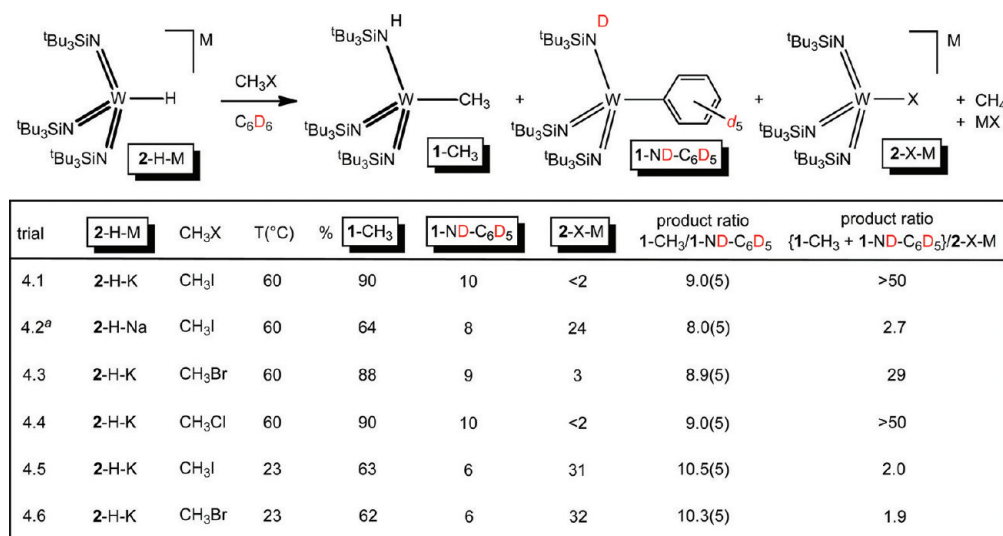
**2. Kinetics of [(tBu<sub>3</sub>SiN)<sub>3</sub>WH]M (2-H-M) and MeX.** Some limited kinetics data were obtained for reactions of [(tBu<sub>3</sub>SiN)<sub>3</sub>WH]M (2-H-M) and MeX (X = Cl, Br, I) at 60.0(4) °C in C<sub>6</sub>D<sub>6</sub> (Table 2). The kinetics runs were subject to two experimental problems: (1) the salt derived from the reduction caused shimming difficulties during <sup>1</sup>H NMR spectroscopic monitoring, and (2) the only integrable signal was a tungsten hydride satellite resonance of 2-H-M, which became very weak after ~2 half-lives. The central W–H resonance for both 2-H-M (M = Na, K) was obscured by residual solvent, and the signal pertaining to the tBu<sub>3</sub>Si group was clustered with the products.

The experiments were conducted under pseudo-first-order conditions, and plots of ln([2-H-K]/[2-H-K]<sub>0</sub>) were linear, whereas second-order plots were decidedly nonlinear. Varia-

Scheme 3



Scheme 4

Table 2. Rate Constants for the Reaction between [(<sup>t</sup>Bu<sub>3</sub>SiN=)<sub>3</sub>WH]M (2-H-M; M = Na, K) and MeX (X = Cl, Br, I) at 60.0(4) °C in Benzene-*d*<sub>6</sub>

expt <sup>b</sup>	[2-MH] <sub>0</sub> (mM)	[CH <sub>3</sub> X] <sub>0</sub> (mM)	amt of CH <sub>3</sub> X (equiv)	no. of half-lives	k <sub>obs</sub> (10 <sup>5</sup> s <sup>-1</sup> )	k (10 <sup>4</sup> M <sup>-1</sup> s <sup>-1</sup> ) <sup>a</sup>
(1) 2-H-K + CH <sub>3</sub> I	15	150	10	3	16.1(6)	10.7(4)
(2) 2-H-K + CH <sub>3</sub> I	15	300	20	3.5	25.1(9)	8.4(3)
(3) 2-H-Na + CH <sub>3</sub> I	15	150	10	1	3.6(3)	2.4(2)
(4) 2-H-Na + CH <sub>3</sub> I	16	368	23	3	6.9(2)	1.88(5)
(5) 2-H-K + CH <sub>3</sub> Br	15	480	32	3	43(1)	9.0(2)
(6) 2-H-K + CH <sub>3</sub> Cl <sup>c</sup>	11	110	10	1	0.8(1)	0.7(1)

<sup>a</sup> Assumes the order in CH<sub>3</sub>X is 1: i.e., k<sub>obs</sub> = k[CH<sub>3</sub>X]. <sup>b</sup> Average of three NMR tube experiments run simultaneously, unless noted otherwise. <sup>c</sup> Single NMR tube experiment.

tions of [CH<sub>3</sub>I] in runs 1–4, while limited, provided data consistent with a non-zero-order dependence on [CH<sub>3</sub>I]; therefore an order of 1 was assumed for all CH<sub>3</sub>X. The average second-order rate constant for CH<sub>3</sub>I and 2-H-K is [9.7(20)] × 10<sup>-4</sup> M<sup>-1</sup> s<sup>-1</sup>, which was roughly 4–5 times faster than the

average of methyl iodide and the sodium congener 2-H-Na ([2.14(34)] × 10<sup>-4</sup> M<sup>-1</sup> s<sup>-1</sup>). Recall that reactions with 2-H-Na tend to produce more halide adduct (i.e., 2-X-Na), and it may be that capture of the tungsten center by NaX during the reduction process is more competitive than the related

scavenging by KX. The single set of runs with 2-H-K and CH<sub>3</sub>Br afford a rate constant comparable with that of methyl iodide, but the limited data on CH<sub>3</sub>Cl suggest that it is roughly an order of magnitude slower. This very modest trend  $I \geq Br > Cl$  is expected for various processes such as nucleophilic hydride delivery, electron transfer, and even a radical process and does not provide detailed mechanistic information.<sup>31</sup>

**Structure of (<sup>t</sup>Bu<sub>3</sub>SiNH)(<sup>t</sup>Bu<sub>3</sub>SiN=)<sub>2</sub>WCH<sub>3</sub> (1-CH<sub>3</sub>).** A selection of crystallographic and refinement details pertaining to (<sup>t</sup>Bu<sub>3</sub>SiNH)(<sup>t</sup>Bu<sub>3</sub>SiN=)<sub>2</sub>WCH<sub>3</sub> (1-CH<sub>3</sub>) is given in Table

**Table 3. Selected Crystallographic and Refinement Data for (<sup>t</sup>Bu<sub>3</sub>SiN=)<sub>2</sub>(<sup>t</sup>Bu<sub>3</sub>SiNH)WCH<sub>3</sub> (1-CH<sub>3</sub>), (<sup>t</sup>Bu<sub>3</sub>SiN=)<sub>2</sub>(<sup>t</sup>Bu<sub>3</sub>SiNH)W(<sup>c</sup>CHCH<sub>2</sub>CHMe) (1-<sup>c</sup>PrMe), and (<sup>t</sup>Bu<sub>3</sub>SiN=)<sub>2</sub>(<sup>t</sup>Bu<sub>3</sub>SiNH)WCHCCH<sub>2</sub> (1-CHCCH<sub>2</sub>)**

	1-Me	1- <sup>c</sup> PrMe <sup>a</sup>	1-CHCCH <sub>2</sub>
formula	C <sub>37</sub> H <sub>85</sub> N <sub>3</sub> Si <sub>3</sub> W	C <sub>40</sub> H <sub>89</sub> N <sub>3</sub> Si <sub>3</sub> W	C <sub>39</sub> H <sub>85</sub> N <sub>3</sub> Si <sub>3</sub> W
formula wt	840.19	904.28	864.23
space group	P2 <sub>1</sub> /c	P $\bar{1}$	P2 <sub>1</sub> /n
Z	4	4	4
a, Å	22.077(4)	12.906(3)	12.9530(2)
b, Å	12.822(3)	17.735(4)	21.0289(2)
c, Å	17.322(4)	22.474(5)	17.0079(2)
α, deg	90	76.43(3)	90
β, deg	109.91(3)	88.86(3)	92.2291(9)
γ, deg	90	79.59(3)	90
V, Å <sup>3</sup>	4610.3(16)	4916.8(17)	4629.23(10)
ρ <sub>calcd</sub> , g cm <sup>-3</sup>	1.209	1.222	1.241
μ, mm <sup>-1</sup>	2.609	2.451	2.600
temp, K	293(2)	293(2)	173(2)
λ (Å)	0.71073	0.71073	0.71073
R indices (I > 2σ(I)) <sup>b,c</sup>	R1 = 0.0346	R1 = 0.1083	R1 = 0.0423
	wR2 = 0.0730	wR2 = 0.2398	wR2 = 0.0686
R indices (all data) <sup>b,c</sup>	R1 = 0.0578	R1 = 0.2432	R1 = 0.1044
	wR2 = 0.0843	wR2 = 0.3537	wR2 = 0.1005
GOF <sup>d</sup>	1.040	1.045	1.103

<sup>a</sup>Two molecules per asymmetric unit. A diffusely formed and positionally disordered small molecule remote from either compound was treated and refined as four carbon atoms per asymmetric unit, hence the formula weight given. <sup>b</sup>R1 =  $\sum ||F_o| - |F_c|| / \sum |F_o|$ . <sup>c</sup>wR2 =  $[\sum w(|F_o| - |F_c|)^2 / \sum w F_o^2]^{1/2}$ . <sup>d</sup>GOF (all data) =  $[\sum w(|F_o| - |F_c|)^2 / (n - p)]^{1/2}$ ; n = number of independent reflections, p = number of parameters.

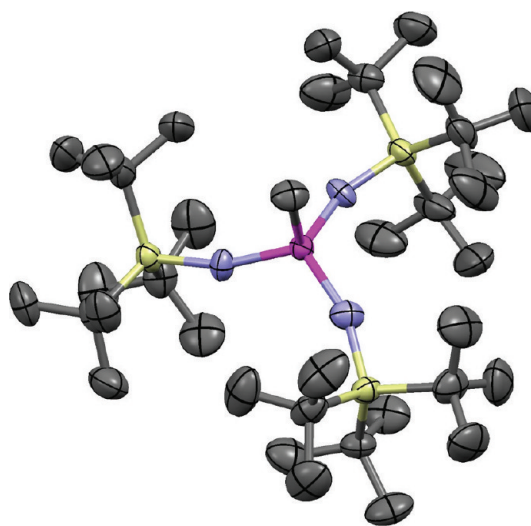
3, important metric parameters are given in Table 4, and a molecular view is presented in Figure 2. The tungsten methyl derivative is a pseudotetrahedral molecule with N–W–C angles that average 103.6(7)° and N–W–N angles that average 114.7(10)°, reflecting the steric requirements of the ligands. Bis-imido-amido derivatives of tungsten are prone to a 3-fold disorder averaging the two bulky ligands, and 1-Me is no exception, as the three  $d(WN)$  values average 1.825(11) Å,<sup>32,33</sup> with W–N–Si angles that average 160.4(8)°. The  $d(WC)$  value is 2.158(6) Å, consistent with a standard sp<sup>3</sup> tungsten–carbon bond.

**[(<sup>t</sup>Bu<sub>3</sub>SiN=)<sub>3</sub>WH]M (2-H-M) and Saturated Alkyl Halides.** 1. *Ethyl Halides.* Utilization of deuterated EtX substrates helped determine whether the site of activation was the same as the site of hydride delivery (Scheme 5). Treatment of [(<sup>t</sup>Bu<sub>3</sub>SiN=)<sub>3</sub>WH]K (2-H-K) with EtI at 100 °C in C<sub>6</sub>D<sub>6</sub> afforded the ethyl complex (<sup>t</sup>Bu<sub>3</sub>SiN=)<sub>2</sub>(<sup>t</sup>Bu<sub>3</sub>SiNH)-

**Table 4. Selected Interatomic Bond Distances (Å) and Angles (deg) for (<sup>t</sup>Bu<sub>3</sub>SiN=)<sub>2</sub>(<sup>t</sup>Bu<sub>3</sub>SiNH)WCH<sub>3</sub> (1-CH<sub>3</sub>), (<sup>t</sup>Bu<sub>3</sub>SiN=)<sub>2</sub>(<sup>t</sup>Bu<sub>3</sub>SiNH)W(<sup>c</sup>CHCH<sub>2</sub>CHMe) (1-<sup>c</sup>PrMe), and (<sup>t</sup>Bu<sub>3</sub>SiN=)<sub>2</sub>(<sup>t</sup>Bu<sub>3</sub>SiNH)WCHCCH<sub>2</sub> (1-CHCCH<sub>2</sub>)**

	1-Me <sup>a</sup>	1- <sup>c</sup> PrMe <sup>a,b</sup>	1-CHCCH <sub>2</sub> <sup>c</sup>
W1–N1	1.815(5)	1.811(14), 1.826(14)	1.782(4)
W1–N2	1.823(5)	1.825(13), 1.83(2)	1.860(4)
W1–N3	1.836(5)	1.837(15), 1.82(2)	1.850(4)
W1–C	2.158(6)	2.21(4), 2.10(4)	2.155(6)
N–Si <sub>av</sub>	1.765(3)	1.73(3)	1.761(6)
N1–W1–N2	114.3(2)	113.7(8), 113.4(9)	111.1(2)
N1–W1–N3	113.9(2)	113.3(8), 112.6(9)	116.5(2)
N2–W1–N3	115.8(2)	115.6(8), 110.3(11)	115.2(2)
N1–W1–C	102.8(2)	103.6(14), 104.2(12)	101.9(2)
N2–W1–C	103.7(2)	99.5(13), 105.7(13)	105.6(2)
N3–W1–C	104.2(2)	109.2(14), 110.2(14)	104.8(2)
W1–N1–Si1	160.1(3)	161.9(13), 169.4(13)	162.6(3)
W1–N2–Si2	161.3(3)	162.3(12), 160.0(16)	157.3(2)
W1–N3–Si3	159.9(3)	162.7(12), 173.3(15)	157.4(3)

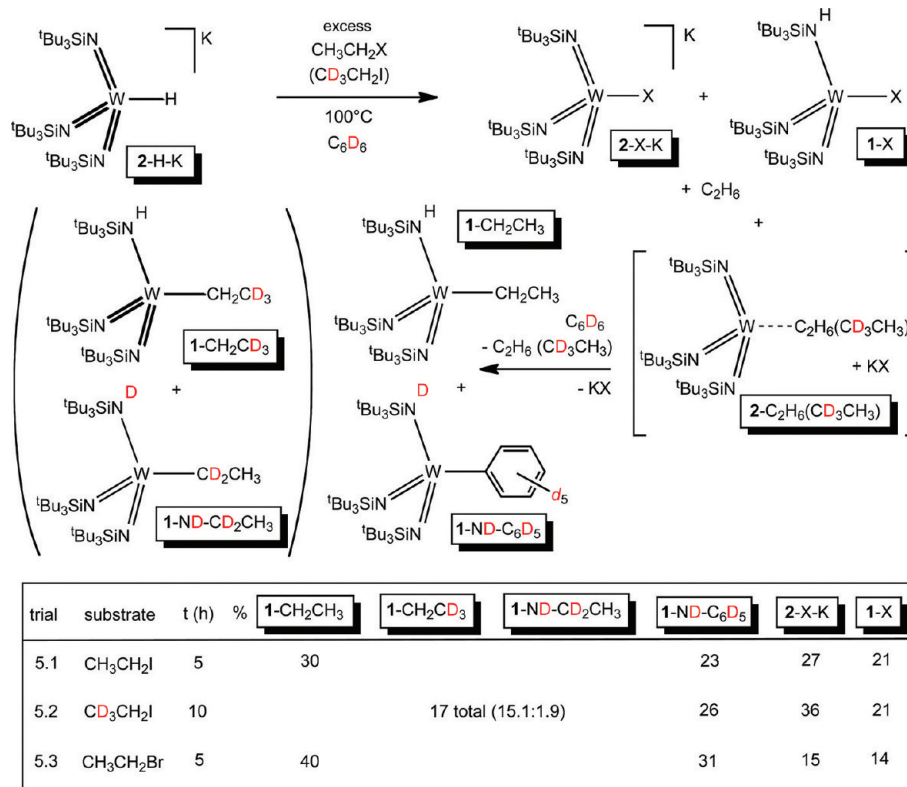
<sup>a</sup>Amide and imide ligands are statistically disordered. <sup>b</sup>Two independent molecules in the asymmetric unit; related parameters from the two molecules are listed together. Cyclopropyl distances are  $d(C1-C2) = 1.46(5)$  Å,  $d(C1-C3) = 1.42(5)$  Å,  $d(C2-C3) = 1.49(5)$  Å, and  $d(C3-C4(Me)) = 1.61(7)$  Å; angles are C3–C1–C2 = 62.1(29)°, C1–C2–C3 = 57.7(26)°, C1–C3–C2 = 60.3(29)°, C1–C3–C4(Me) = 100.6(43)°, and C2–C3–C4(Me) = 105.1(41)°. <sup>c</sup>Allenyl distances are  $d(C1-C2) = 1.183(8)$  Å and  $d(C2-C3) = 1.320(11)$  Å; the W–C1–C2 angle is 125.0(5)°, and the C1–C2–C3 angle is 178.0(10)°.



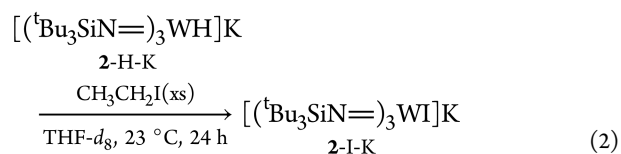
**Figure 2.** Molecular view of (<sup>t</sup>Bu<sub>3</sub>SiNH)(<sup>t</sup>Bu<sub>3</sub>SiN=)<sub>2</sub>WCH<sub>3</sub> (1-CH<sub>3</sub>); note that imido and amido groups are disordered.

WCH<sub>2</sub>CH<sub>3</sub> (1-CH<sub>2</sub>CH<sub>3</sub>) in 30% yield, accompanied by the solvent-activated product (<sup>t</sup>Bu<sub>3</sub>SiND)(<sup>t</sup>Bu<sub>3</sub>SiN=)<sub>2</sub>WC<sub>6</sub>D<sub>5</sub> (1-ND-C<sub>6</sub>D<sub>5</sub>, 23%), the KI adduct [(<sup>t</sup>Bu<sub>3</sub>SiN=)<sub>3</sub>WI]K (2-I-K, 27%), and the neutral iodide (<sup>t</sup>Bu<sub>3</sub>SiN=)<sub>2</sub>(<sup>t</sup>Bu<sub>3</sub>SiNH)WI (1-I, 21%). When CD<sub>3</sub>CH<sub>2</sub>I was used, the amount of 1-I remained constant at 21%, suggesting it was formed by a path, possibly a radical or electron transfer process, different from the one generating the remaining products: i.e., the hydride delivery path. The decline in ethane-activated products with respect to KI adduct upon deuteration is reminiscent of the MeI case discussed above. Both CH- and CD-activated ethane products (17%) are observed, with 1-CH<sub>2</sub>CD<sub>3</sub> dominating over 1-ND-

Scheme 5



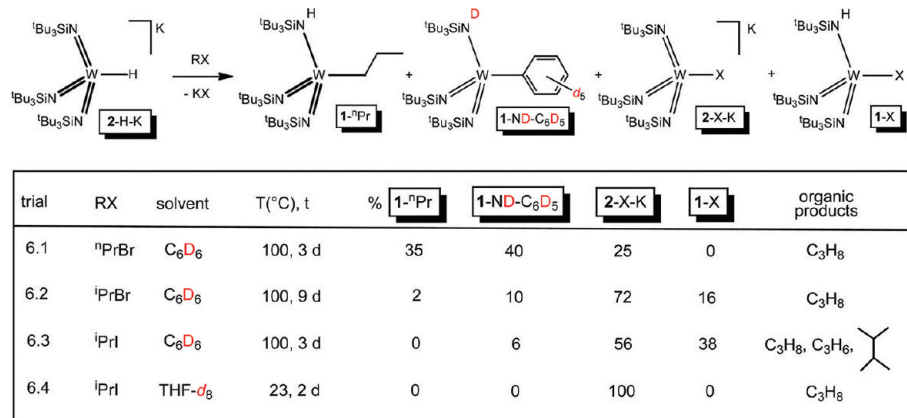
CD<sub>2</sub>CH<sub>3</sub> in a 15.1:1.9 ratio, implicating a  $k_H/k_D$  value of 7.9(3) for activation from an ethane complex intermediate, (<sup>t</sup>Bu<sub>3</sub>SiN=)<sub>3</sub>W(CH<sub>3</sub>CD<sub>3</sub>) (2-CH<sub>3</sub>CD<sub>3</sub>). No scrambling between  $\alpha$  and  $\beta$  sites of the W-CH<sub>2</sub>CD<sub>3</sub> and W-CD<sub>2</sub>CH<sub>3</sub> groups was detected by NMR spectroscopy; thus, it is clear that the hydride was transferred to the CH<sub>2</sub> group of the substrate, and no  $\beta$ -elimination processes that lead to scrambling were evident. The decline in CD<sub>3</sub>CH<sub>3</sub>-activated products relative to 1-ND-C<sub>6</sub>D<sub>5</sub> may be an indication that deuteration weakens the binding in the putative alkane complex intermediates. It is likely the binding of ethane in the (<sup>t</sup>Bu<sub>3</sub>SiN=)<sub>3</sub>W pocket is asymmetric, i.e., fast and reversible (<sup>t</sup>Bu<sub>3</sub>SiN=)<sub>3</sub>W...CH<sub>3</sub>CD<sub>3</sub>  $\leftrightarrow$  (<sup>t</sup>Bu<sub>3</sub>SiN=)<sub>3</sub>W...CD<sub>3</sub>CH<sub>3</sub>; hence, the KIE should be considered a phenomenological value encompassing both preferential binding and activation events.<sup>7</sup> In this sense, if



ethane is more readily lost from (<sup>t</sup>Bu<sub>3</sub>SiN=)<sub>3</sub>W...CD<sub>3</sub>CH<sub>3</sub>, the KIE could be even more skewed in favor of CH activation due to an induced kinetic isotope effect.<sup>34</sup>

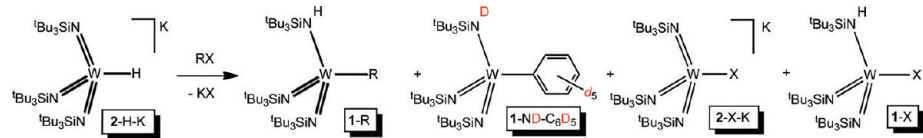
Unlike the methyl cases, the switch from alkyl iodide to CH<sub>3</sub>CH<sub>2</sub>Br (trial 5.3) afforded a significant increase in the amount of activation products—40% 1-CH<sub>2</sub>CH<sub>3</sub> and 31% 1-ND-C<sub>6</sub>D<sub>5</sub>—relative to 2-Br-K and 1-Br. The diminished amount of 1-Br still fits with its generation via a separate

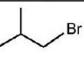
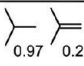
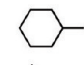
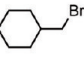
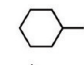
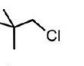

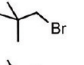

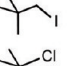
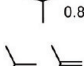
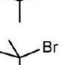
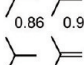
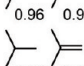
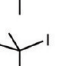
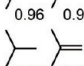
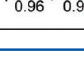

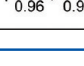
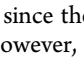
Scheme 6





Scheme 7



trial	RX	solvent	T(°C), t	% 1-R	1-ND-C <sub>6</sub> D <sub>5</sub>	2-X-K	1-X	organic products <sup>a</sup>
7.1		C <sub>6</sub> D <sub>6</sub>	100, 3 d	0	31	54	15	 0.97,  0.21
7.2		C <sub>6</sub> D <sub>6</sub>	150, 24 h	0	10	84	6	
7.3 <sup>b</sup>		C <sub>6</sub> D <sub>6</sub>	150, 36 h	0	0	100	0	
7.4		C <sub>6</sub> D <sub>6</sub>	100, 9 d	0	6	63	31	 1.06
7.5		C <sub>6</sub> D <sub>6</sub>	100, 3 d	0	0	25	75	 0.81
7.6		C <sub>6</sub> D <sub>6</sub>	60, 8 h	0	20	2	78	 0.86,  0.98
7.7		C <sub>6</sub> D <sub>6</sub>	60, 8 h	0	14	0	86	 0.96,  0.94
7.8		C <sub>6</sub> D <sub>6</sub>	60, 3 h	0	14	0	86	 0.96,  0.94

path, and its decline may be the origin of the greater amount of other products. Note that the ratio of 1-CH<sub>2</sub>CH<sub>3</sub>:1-ND-C<sub>6</sub>D<sub>5</sub> is essentially independent of X, perhaps another indication that solvent activation derives from RH loss from (t-Bu<sub>3</sub>SiN=)<sub>3</sub>W(RH) (2-RH). It is difficult to spot a correlation in the production of 1-X to other species, hence more alkyl halides were scrutinized.

The addition of EtI to 2-H-K in THF-*d*<sub>8</sub> at 23 °C provided 100% [(t-Bu<sub>3</sub>SiN=)<sub>3</sub>WI]K (2-I-K) according to eq 2. It appears that the combination of a larger substrate and donor solvent drives the reaction toward KI adduct formation.

**2. Propyl Halides.** Higher temperatures were necessary for reasonable rates when propyl halide substrates were explored in reactions with [(t-Bu<sub>3</sub>SiN=)<sub>3</sub>WH]K (2-H-K), as shown in Scheme 6. With <sup>n</sup>PrBr, 75% activation products were produced, with the distribution roughly equal between (t-Bu<sub>3</sub>SiN=)<sub>2</sub>(t-Bu<sub>3</sub>SiNH)W<sup>n</sup>Pr (1-<sup>n</sup>Pr, 35%) and C<sub>6</sub>D<sub>6</sub>-activation product (t-Bu<sub>3</sub>SiND)(t-Bu<sub>3</sub>SiN=)<sub>2</sub>WC<sub>6</sub>D<sub>5</sub> (1-ND-C<sub>6</sub>D<sub>5</sub>, 40%). The remaining 25% was [(t-Bu<sub>3</sub>SiN=)<sub>3</sub>WBr]K (2-Br-K), and no detectable 1-Br was noted. No secondary activation of propane was indicated, and use of <sup>i</sup>PrBr and <sup>i</sup>PrI also failed to elicit an isopropyl tungsten compound. Instead, isopropyl bromide generated a small amount of 1-<sup>n</sup>Pr (2%), about 10% of the solvent-activated complex 1-ND-C<sub>6</sub>D<sub>5</sub>, and 72% of the major product, the KBr adduct 2-Br-K. In addition, 16% of (t-Bu<sub>3</sub>SiN=)<sub>2</sub>(t-Bu<sub>3</sub>SiNH)WBr (1-Br) was observed, and this increased to 38% when isopropyl iodide was the substrate. With the latter, no 1-<sup>n</sup>Pr was produced and the remainder of the material was 2-I-K (56%) and 1-ND-C<sub>6</sub>D<sub>5</sub> (6%). Accompanying 1-Br were propane, propene, and 2,3-dimethylbutane, products that are suggestive of a radical process, since they can be derived from <sup>i</sup>Pr radical. In THF-*d*<sub>8</sub>, the combination of 2-H-K and <sup>i</sup>PrI afforded 100% 2-I-K, akin to the related experiment with EtI (eq 2).

The premise that 1-R and 1-ND-C<sub>6</sub>D<sub>5</sub> originate from a common—or set of common—intermediates is called into

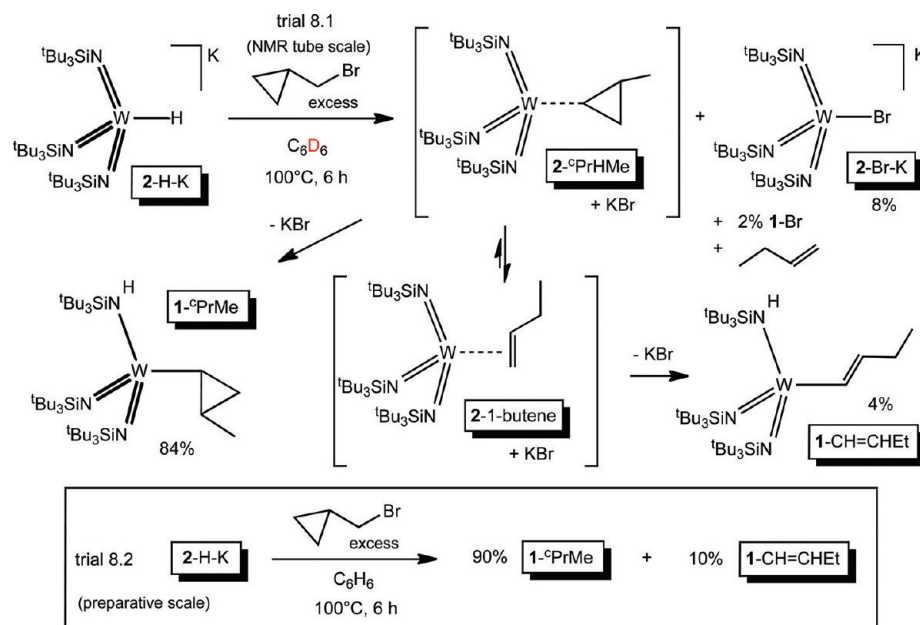
question by trials 6.1 and 6.2, since the 1-<sup>n</sup>Pr/1-ND-C<sub>6</sub>D<sub>5</sub> ratio is dependent on substrate. However, this is the first case that differential alkane binding is not caused by deuteration—in this instance primary CH vs secondary CH—and loss of propane from different sites may play a role. It is plausible that propane is more easily lost from a secondary binding site, i.e., W(η<sup>2</sup>-H<sub>2</sub>C(CH<sub>3</sub>)<sub>2</sub>), and this is the initial binding mode generated upon hydride delivery; provided propane loss is competitive with migration to the methyl termini, the scenario of a common set of intermediates could still be satisfied.

### 3. Secondary, Tertiary, and Hindered Saturated Halides.

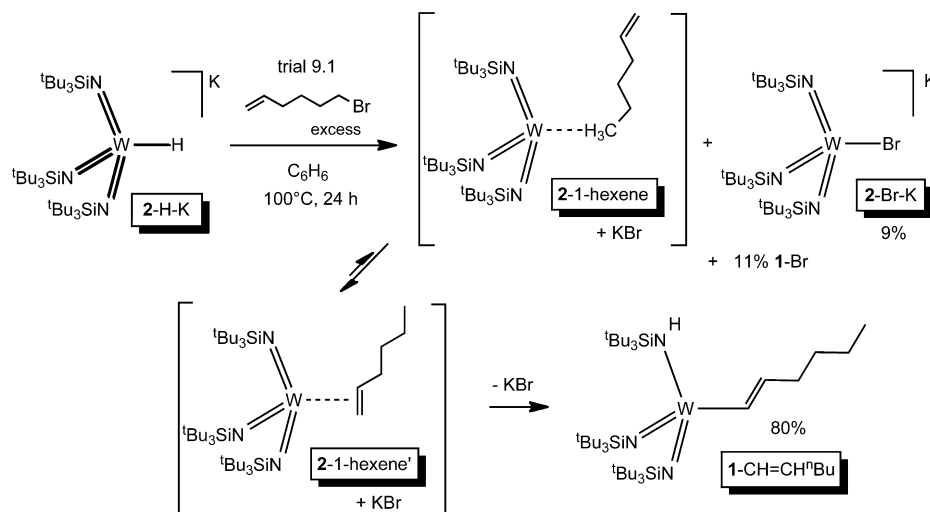
Given the results with <sup>n</sup>PrX, other secondary halides, tertiary halides, and hindered primary substrates were examined to see if any (t-Bu<sub>3</sub>SiN=)<sub>2</sub>(t-Bu<sub>3</sub>SiNH)WR (1-R) could be observed upon exposure to [(t-Bu<sub>3</sub>SiN=)<sub>3</sub>WH]K (2-H-K). Scheme 7 reveals that for isobutyl bromide and cyclohexylmethyl bromide, no tungsten alkyl product was observed, but the amounts of (t-Bu<sub>3</sub>SiND)(t-Bu<sub>3</sub>SiN=)<sub>2</sub>WC<sub>6</sub>D<sub>5</sub> (1-ND-C<sub>6</sub>D<sub>5</sub>) and [(t-Bu<sub>3</sub>SiN=)<sub>3</sub>WBr]K (2-Br-K) were greater than that of (t-Bu<sub>3</sub>SiN=)<sub>2</sub>(t-Bu<sub>3</sub>SiNH)WBr (1-Br), a result accommodated by either hydride delivery or radical chain paths. A switch to <sup>neo</sup>PeX substrates again gave no 1-<sup>neo</sup>Pe, but more 1-X was produced for X = I vs X = Br, and use of 2-H-Na and <sup>neo</sup>PeCl afforded only 2-Cl-Na. t-BuX substrates provided mostly 1-X, no 1-R, and a lesser amount of 1-ND-C<sub>6</sub>D<sub>5</sub>, consistent with a shift to a radical path, replete with isobutene and isobutylene as organic products. As steric factors are increased, hydride delivery appears to become the minor path and radical mechanisms start to dominate.

**4. Radical Probes.** Given the switch to potential radical-based mechanism(s) as steric factors increase, and as secondary and tertiary substrates were introduced, two radical probes were investigated.<sup>35–37</sup> The rate constant for the rearrangement of cyclopropylmethyl radical to 3-butenyl radical is 8.6 × 10<sup>7</sup> s<sup>−1</sup> at 25 °C;<sup>35,36</sup> hence, cyclopropylmethyl bromide was chosen as a substrate with the potential to ferret out radical character. As

Scheme 8



Scheme 9



Scheme 8 illustrates, a 10-fold excess of substrate with **2-H-K** in  $C_6D_6$  for 6 h at 100 °C afforded mostly (84%) the nonrearranged alkyl product  $(tBu_3SiN)_2(tBu_3SiNH)W-PrMe$  (**1-PrMe**), and the activation occurred solely at a nonmethylated secondary cyclopropyl site rather than the methyl. Multidimensional NMR correlation techniques positively identified the conformation, which was ultimately confirmed by an X-ray crystallographic study, albeit one with poor-quality data. A minor product (4%) in the process was the rearrangement product  $(tBu_3SiN)_2(tBu_3SiNH)W(trans-CH=CHEt)$  (**1-CH=CHEt**), but **1-Br** (2%) was also formed; hence, the possibility exists that **1-CH=CHEt** was derived solely from a *separate* radical path.

Upon scale-up of the reaction in benzene (trial 8.2),  $^1H$  NMR analysis of the crude reaction mixture showed no **1-Br** or **2-Br-K**, yet 10% rearrangement occurred along with 90% unrearranged **1-PrMe** (52% isolated yield). Since the lack of an *observed amount* of **1-Br** does not completely rule out radical paths, any such path would require hydride abstraction on a

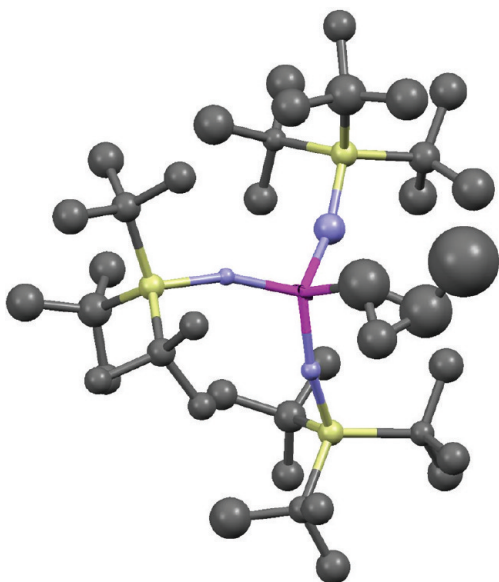
time scale roughly on par with that of rearrangement at 100 °C ( $\sim 10^{10} s^{-1}$ ).<sup>35,36</sup> Unfortunately, while rearrangement of cyclopropylmethyl radical is fast, so is the rearrangement of cyclopropylmethyl cation; hence, it seems reasonable that the Lewis acidity of the tungsten center could also effect some rearrangement. Given the predominance of unrearranged product, dominance of a hydride delivery path is certainly reasonable. Note that both alkane complex intermediates, unrearranged **2-H<sup>o</sup>PrMe** and rearranged **2-1-butene**, are activated at  $sp^2$  carbons, at a ring site anti to the methyl in the former and at the *trans*-alkene terminus in the latter, thereby reflecting selectivity patterns previously observed in early-metal imido 1,2-RH additions.<sup>20,23,38</sup>

A second radical probe, albeit a significantly slower one, is the 5-hexenyl radical, which rearranges to the cyclopentylmethyl radical with a unimolecular rate of  $2.0 \times 10^5 s^{-1}$  at 25 °C.<sup>35,37</sup> No rearrangement product is observed in this instance, consistent with the rate discussion above, and the tungsten  $sp^2$ -activated alkyl  $(tBu_3SiN)_2(tBu_3SiNH)W(trans-CH=$

CH<sup>n</sup>Bu) (1-CH=CH<sup>n</sup>Bu) was identified in the crude reaction mixture in 80% yield. The remaining constituents are 2-Br-K (9%) and 1-Br (11%). Since (tBu<sub>3</sub>SiN=)<sub>2</sub>(tBu<sub>3</sub>SiNH)-WCH<sub>2</sub><sup>c</sup>Pe (1-CH<sub>2</sub><sup>c</sup>Pe) was previously shown to be stable to the reaction conditions,<sup>30</sup> the most likely scenario for the production of 1-CH=CH<sup>n</sup>Bu is illustrated in Scheme 9. Hydride delivery by 2-H-K affords a 1-hexene adduct, 2-1-hexene, that is activated at its sp<sup>2</sup> carbon end after migration down the alkyl chain.<sup>20,23,38</sup>

#### 5. Structure of (tBu<sub>3</sub>SiN=)<sub>2</sub>(tBu<sub>3</sub>SiNH)W-<sup>c</sup>PrMe (1-<sup>c</sup>PrMe).

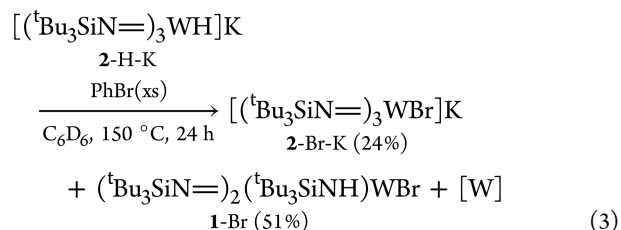
An X-ray crystallographic study of (tBu<sub>3</sub>SiN=)<sub>2</sub>(tBu<sub>3</sub>SiNH)-W-<sup>c</sup>PrMe (1-<sup>c</sup>PrMe) was undertaken, and details of the crystallographic and data refinement can be found in Table 3, while metric parameters are given in Table 4. It was a poor data set, and an isotropic model was the most appropriate solution to the refinement. One of the two independent molecules in the asymmetric unit was rife with disorder in the peripheral tBu groups; thus, Figure 3 depicts the least problematic structure.



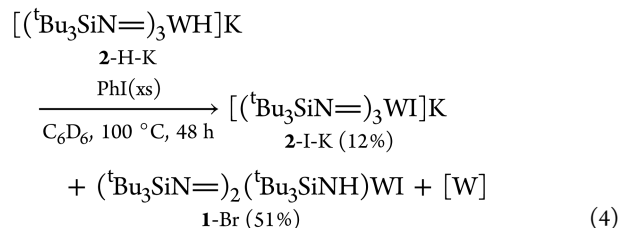
**Figure 3.** Molecular view of the less disordered of two independent molecules of (tBu<sub>3</sub>SiN=)<sub>2</sub>(tBu<sub>3</sub>SiNH)W-<sup>c</sup>PrMe (1-<sup>c</sup>PrMe); data quality led to an isotropic refinement.

Although the thermal parameters of its methylcyclopropyl carbons were large, the model was good enough to confirm that the Me and W were disposed anti about the cyclopropane ring, as shown by the multidimensional NMR studies. Despite the crystallographic problems, the core values were normal, with the usual imide and amide disorder:  $d(\text{WN})_{\text{av}} = 1.824(13)$  Å,  $d(\text{W-C})_{\text{av}} = 2.16(8)$  Å;  $\angle \text{NWN}_{\text{av}} = 113.2(17)^\circ$ ,  $\angle \text{CWN}_{\text{av}} = 105(4)^\circ$ .

**[(tBu<sub>3</sub>SiN=)<sub>3</sub>WH]M (2-H-M) and Unsaturated Substrates.** 1. *sp*<sup>2</sup>-Carbon Halides. Since (tBu<sub>3</sub>SiND)-(tBu<sub>3</sub>SiN=)<sub>2</sub>WC<sub>6</sub>D<sub>5</sub> (1-ND-C<sub>6</sub>D<sub>5</sub>) was a typical byproduct in many of the studies discussed, PhX was a logical substrate. Treatment of [(tBu<sub>3</sub>SiN=)<sub>3</sub>WH]K (2-H-K) with PhBr at 150 °C for 24 h produced 51% (tBu<sub>3</sub>SiN=)<sub>2</sub>(tBu<sub>3</sub>SiNH)WBr (1-Br), 24% [(tBu<sub>3</sub>SiN=)<sub>3</sub>WBr]K (2-Br-K), and unidentified tungsten products (eq 3). A switch to PhI enabled reduction to occur at lower temperatures, and [(tBu<sub>3</sub>SiN=)<sub>3</sub>WI]K (2-I-K, 12%) and (tBu<sub>3</sub>SiN=)<sub>2</sub>(tBu<sub>3</sub>SiNH)WI (1-I, 51%) were generated along with a set of resonances in the <sup>1</sup>H NMR



spectrum consistent with the formulation [(tBu<sub>3</sub>SiN=)<sub>3</sub>WPh]K (2-K-Ph, 22%,  $\delta$  1.43 (s, 81 H), 6.59 (t, 8 Hz, *p*-H), 6.80 (t, 8 Hz, *m*-H), 8.40 (d, 8 Hz, *o*-H)) (eq 4). The spectral



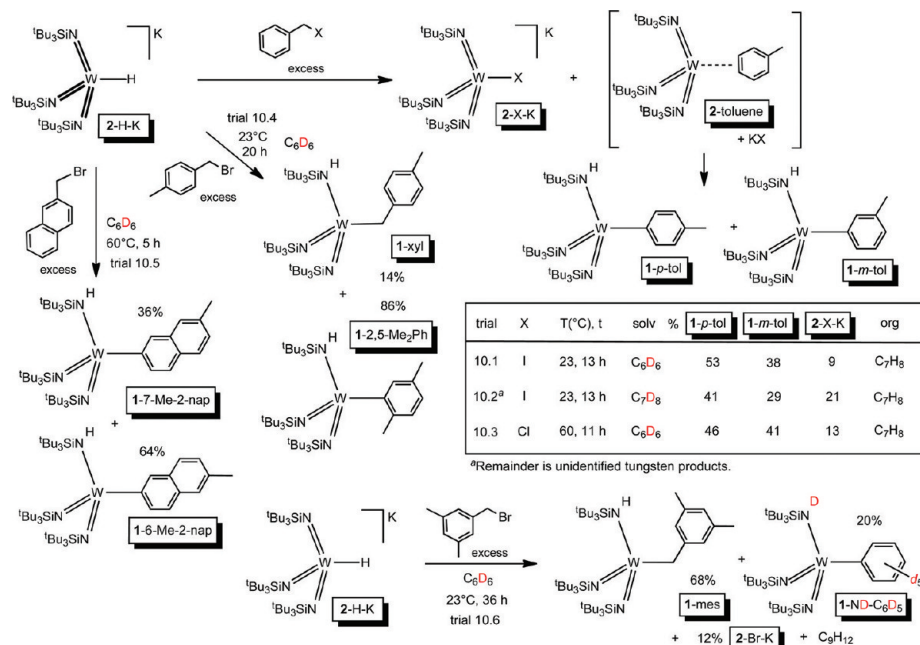
characteristics were similar to those of [(tBu<sub>3</sub>SiN=)<sub>3</sub>WPh]Li (2-Li-Ph), but without independent synthesis, assignment of this minor product remains tentative. The most likely arene activation products, (tBu<sub>3</sub>SiNH)(tBu<sub>3</sub>SiN=)<sub>2</sub>WPh (1-Ph) and 1-ND-C<sub>6</sub>D<sub>5</sub>, were not discerned in the product mixture.

Previous studies in d<sup>0</sup> RH activation have shown a selectivity for sp<sup>2</sup> over sp<sup>3</sup> CH bonds,<sup>20,23,38</sup> a factor that presumably determined the 1,2-RH addition of a cyclopropyl CH rather than a methyl CH in Scheme 8 and a vinylic CH rather than an aliphatic CH in Scheme 9. When [(tBu<sub>3</sub>SiN=)<sub>3</sub>WH]K (2-H-K) was treated with vinyl bromide, a reaction occurred at a reasonable rate only at high temperatures (140 °C) over several days, producing a multitude of unidentified products. Even 2-Br-K and 1-Br were not positively identified. Vinyl halides have reaction paths such as insertion<sup>30</sup> and polymerization that are not available to other substrates, and these may supersede hydride delivery paths, producing complexes that have not been prepared by other means.

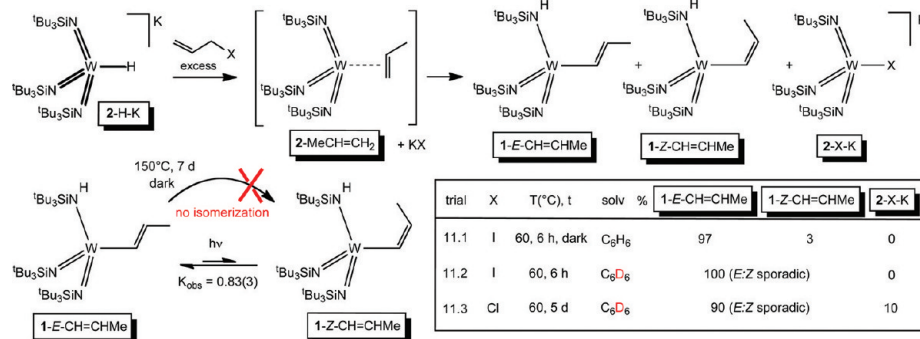
**2. Benzylic and Allylic Halides.** A smattering of benzylic substrates were evaluated, and consistent with previously noted selectivities,<sup>20,23,38</sup> aryl CH bond activation predominated.<sup>39,40</sup> As Scheme 10 illustrates, exposure of [(tBu<sub>3</sub>SiN=)<sub>3</sub>WH]K (2-H-K) with BnI at 23 °C for 13 h in benzene-*d*<sub>6</sub> afforded two aryl activation products, (tBu<sub>3</sub>SiNH)(tBu<sub>3</sub>SiN=)<sub>2</sub>W(C<sub>6</sub>H<sub>4</sub>-*p*-Me) (1-*p*-tol, 53%) and 38% (tBu<sub>3</sub>SiNH)(tBu<sub>3</sub>SiN=)<sub>2</sub>W-(C<sub>6</sub>H<sub>4</sub>-*m*-Me) (1-*m*-tol, 38%), along with 9% of [(tBu<sub>3</sub>SiN=)<sub>3</sub>WI]K (2-I-K) and trace toluene. No activation of the benzylic position was observed, consistent with the known preference for aryl over benzyl 1,2-RH addition. The same reaction when carried out in toluene-*d*<sub>8</sub> yielded essentially the same ratio of toluene-activated products but an increased amount of 2-I-K (21%); most importantly, no (<3%) activation of C<sub>7</sub>D<sub>8</sub> was noted. A switch to BnCl as the substrate and a change in conditions (60 °C, 11 h) provided a 46/41 ratio of para to meta activation products and 13% 2-Cl-K.

In the case of xylol bromide (trial 10.4), benzylic activation was observed, as treatment of 2-H-K with BrCH<sub>2</sub>C<sub>6</sub>H<sub>4</sub>-*p*-CH<sub>3</sub> at 23 °C for 20 h afforded 14% (tBu<sub>3</sub>SiNH)(tBu<sub>3</sub>SiN=)<sub>2</sub>W-(CH<sub>2</sub>C<sub>6</sub>H<sub>4</sub>-*p*-Me) (1-xyl) in addition to the major (86%) aryl-activated product (tBu<sub>3</sub>SiNH)(tBu<sub>3</sub>SiN=)<sub>2</sub>W(C<sub>6</sub>H<sub>3</sub>-2,5-Me<sub>2</sub>)

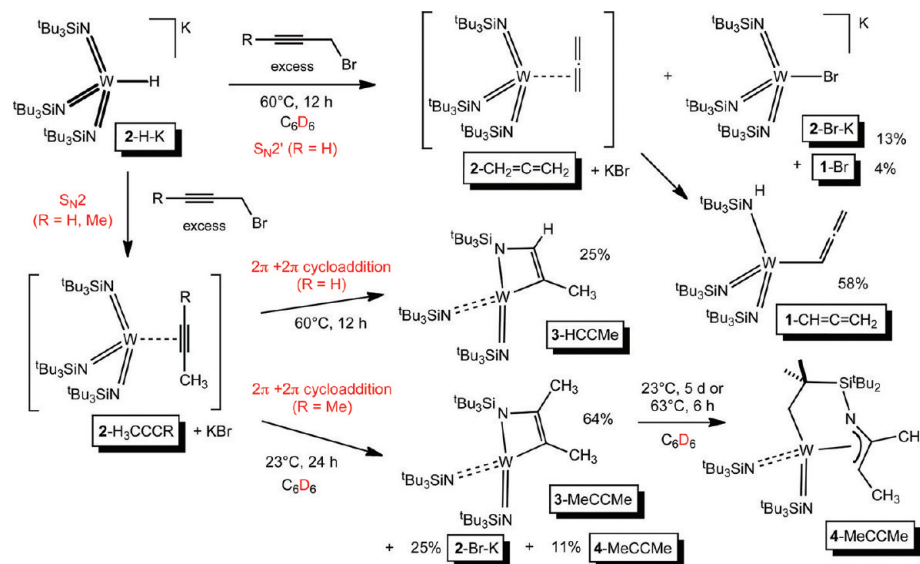
Scheme 10



Scheme 11



Scheme 12



(1-2,5-Me<sub>2</sub>Ph). No solvent, i.e., benzene-*d*<sub>6</sub>, activation or halide adduct formation was seen; hence, this case is an unusual

example where the products are solely due to CH bond activation. A similar result was obtained for apparent hydride



transfer from 2-H-K to 2-bromomethylnaphthalene at 60 °C for 5 h in  $C_6D_6$  (trial 10.5), where only the 2-naphthalenyl derivatives  $(^tBu_3SiNH)(^tBu_3SiN=)_2W(2-C_{10}H_6-6-Me)$  (1-6-Me-2-nap) and  $(^tBu_3SiNH)(^tBu_3SiN=)_2W(2-C_{10}H_6-7-Me)$  (1-7-Me-2-nap) are formed in a  $\sim 16/9$  ratio. In the case of the hindered benzylic substrate mesityl bromide, solvent activation—in this case formation of 20%  $(^tBu_3SiND)(^tBu_3SiN=)_2WC_6D_5$  (1-ND- $C_6D_5$ ) from  $C_6D_6$ —reemerged as a component in the reaction, and 68% of the product mixture was due to benzylic activation of mesitylene, as evidenced by identification of  $(^tBu_3SiNH)(^tBu_3SiN=)_2WCH_2C_6H_4-3,5-Me_2$  (1-mes). The halide adduct 2-Br-K was formed in 12% yield, and a trace of mesitylene was noted.

In Scheme 11, the treatment of  $[(^tBu_3SiN=)_3WH]K$  (2-H-K) with  $H_2C=CHCH_2X$  is shown, and both the *E* and *Z* isomers of propenyl activation,  $(^tBu_3SiNH)(^tBu_3SiN=)_2W(E-CH=CHMe)$  (1-*E*-CH=CHMe) and  $(^tBu_3SiNH)(^tBu_3SiN=)_2W(Z-CH=CHMe)$  (1-*Z*-CH=CHMe) are the products, with no other species formed when  $X = I$ . For  $X = Cl$ ,  $\sim 10\%$  2-Cl-K is also generated. It is not clear whether any 1-*Z*-CH=CHMe is derived directly from activation, as the *E/Z* ratio was found to be dependent on the amount of exposure to room light. Subsequent studies revealed that the *cis* isomer is produced in about 45% yield at 23 °C in a photostationary state under ambient conditions, and extended thermolysis of 1-*E*-CH=CHMe in the dark failed to generate any 1-*Z*-CH=CHMe. Once again,  $sp^2$  activation was preferred over allylic activation;<sup>20,23,38</sup> hence, the plausible propene adducts of tris-imido tungsten appear to activate from a single conformation.

The examination of propargylic substrates provided evidence of diversion from the standard reactivity of the previous substrates. As Scheme 12 shows, treatment of  $[(^tBu_3SiN=)_3WH]K$  (2-H-K) with 3-bromopropyne at 60 °C for 24 h in  $C_6D_6$  gives 13% of the halide adduct  $[(^tBu_3SiN=)_3WBr]K$  (2-Br-K), a small amount of  $(^tBu_3SiN=)_2(^tBu_3SiNH)WBr$  (1-Br, 4%), and 58% of the allene-activated complex  $(^tBu_3SiN=)_2(^tBu_3SiNH)WCH=C=CH_2$  (1-CH=C=CH<sub>2</sub>). The last species is consistent with an  $S_N2'$  delivery of hydride by 2-H-K to provide an intermediate allene complex,  $(^tBu_3SiN=)_3W(allene)$  (2- $H_2C=C=CH_2$ ), from which CH activation occurs. Since 1-CH=C=CH<sub>2</sub> was the major product, the reaction was scaled up and the allenyl species<sup>41,42</sup> was isolated as a yellow powder in 31% yield. A strong, sharp infrared band at  $1915\text{ cm}^{-1}$  was assigned to the asymmetric CCC mode common to allenic units, and  $^1H$  NMR resonances ( $C_6D_6$ , Table 1) at  $\delta$  6.70 (t, 7 Hz,  $^2J_{WH} = 7\text{ Hz}$ , 1H) and  $\delta$  4.35 (d, 7 Hz,  $^4J_{WH} = 7\text{ Hz}$ , 2H) were assigned to the CH and CH<sub>2</sub> hydrogens. The  $^{13}C\{^1H\}$  NMR spectrum was also diagnostic, with a resonance at  $\delta$  109.08 accompanied by  $^1J_{WC} = 179\text{ Hz}$  indicative of the  $\alpha$ -carbon and resonances at  $\delta$  212.07 and  $\delta$  67.08 ( $^3J_{WC} = 8\text{ Hz}$ ) consistent with the  $sp$  and  $sp^2$  carbons, respectively. Spectral characteristics for 1-CH=C=CH<sub>2</sub> closely matched those of  $Cp(CO)_3WCH=C=CH_2$ ,<sup>41</sup> although its  $^1J_{WC}$  value of 47 Hz is attenuated due to its higher coordination number and correspondingly less tungsten  $s$  character in the  $W-C(\alpha)$  bond.

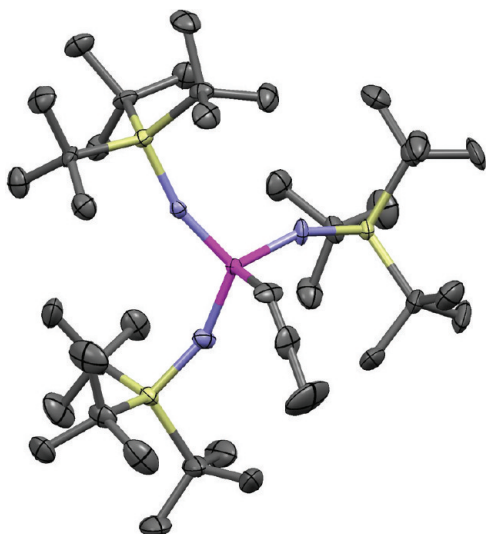
In the reaction with propargyl bromide,  $S_N2$  hydride delivery was expected to generate an intermediate propyne adduct,  $(^tBu_3SiN=)_3W(H_3CCCH)$  (2-HCCCH<sub>3</sub>), but instead of  $sp$  CH activation,  $2\pi + 2\pi$  cycloaddition occurred to provide a tungstaazacyclobutene,  $(^tBu_3SiN=)_2W(\kappa-N,C-N(Si^tBu_3)CHC(Me)-)$  (3-HCCMe) as the remaining product. Coupled

resonances at  $\delta$  2.62 (d, 2 Hz, 3H) and  $\delta$  5.89 (q, 2 Hz, 1H), and a large  $^3J_{WH}$  value of 54 Hz accompanying the latter, were indicative of a trans three-bond linkage between tungsten and the proton.

Competition between CH activation and cycloaddition has been previously observed in titanium<sup>19,43</sup> and related vanadium systems, and the latter underwent ring expansion reactions.<sup>25,26</sup> When bromo-2-butyne was the substrate, the  $S_N2'$  path was not observed, presumably due to steric hindrance of hydride delivery to methyl-containing alkyne carbon, and only the tungstacycle  $(^tBu_3SiN=)_2W(\kappa-N,C-N(Si^tBu_3)C(Me)C(Me)-)$  (3-MeCCMe, 64%) and a rearrangement product (11%) were found after 24 h at 23 °C ( $C_6D_6$ ) in addition to 2-Br-K (25%). The  $^1H$  NMR spectrum of 3-MeCCMe resulted in one sharp resonance at  $\delta$  1.33 (54 H) and one broad resonance at  $\delta$  1.21 (27 H), which were assigned to the free and cyclized imido ligands, in addition to those of the minor rearrangement product. When the temperature was raised to 70 °C, the  $\delta$  1.21 resonance sharpened, consistent with restricted rotation of the  $^tBu$  groups in the metallacycle. Distinct Me resonances ( $\delta$  2.28 and  $\delta$  2.52 ( $^3J_{WH} = 13\text{ Hz}$ )) were observed by  $^1H$  NMR spectroscopy, and two methyl ( $\delta$  15.81 ( $^3J_{WC} = 26\text{ Hz}$ ),  $\delta$  20.71 ( $^2J_{WC} = 9\text{ Hz}$ )) and two alkenyl ( $\delta$  126.23 ( $^2J_{WC} = 15\text{ Hz}$ ),  $\delta$  174.24 ( $^1J_{WH} = 161\text{ Hz}$ )) carbon resonances were observed by  $^{13}C\{^1H\}$  NMR spectroscopy. These did not change upon warming; thus, reversible formation of the metallacycle is not facile. No attempts to separate 3-MeCCMe from its rearrangement product were attempted.

Thermolysis of 3-MeCCMe for 6 h at 63 °C caused complete conversion to the rearrangement product, the cyclometalated azaallyl  $(^tBu_3SiN=)_2W(\kappa-C,\eta^3-C,N-CH_2CMe_2Si(^tBu_2)NCMeCHMe)$  (4-MeCCMe), analogous to similar rearrangements derived from 2-butyne and 3-hexyne additions to  $(^tBu_3SiN=)_2(^tBu_3SiNH)V(OEt_2)$ .<sup>25,26</sup> NMR spectroscopic characterization of azaallyl 4-MeCCMe revealed inequivalent  $Si^tBu_3$ ,  $^tBu$ ,  $CMeMe$ , and  $CHH$  groups, consistent with the asymmetry derived from the facial binding of the azaallyl fragment (Table 1). In the  $^{13}C\{^1H\}$  NMR spectrum, tungsten couplings to the azaallyl carbons at  $\delta$  53.28 (NCC,  $J_{WC} = 24\text{ Hz}$ ) and  $\delta$  180.47 (NC,  $J_{WC} = 10\text{ Hz}$ ) were modest in comparison to coupling with the metallacyclic methylene ( $\delta$  54.08 ( $J_{WC} = 105\text{ Hz}$ )), consistent with the  $\pi$  character of the tungsten-azaallyl bonding. While 4-MeCCMe was only characterized by NMR spectroscopy, its strong spectral parallels to the structurally characterized vanadium example lend credence to the posited geometry shown in Scheme 12.

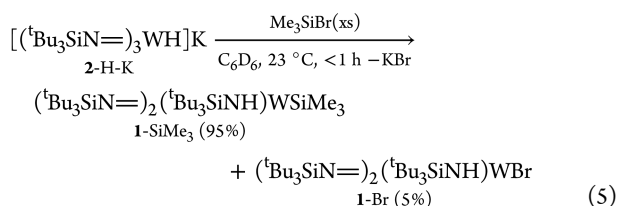
**3. Structure of  $(^tBu_3SiN=)_2(^tBu_3SiNH)WCH=C=CH_2$  (1-CH=C=CH<sub>2</sub>).** An X-ray crystal structure determination of  $(^tBu_3SiN=)_2(^tBu_3SiNH)WCH=C=CH_2$  (1-CH=C=CH<sub>2</sub>) was conducted, and a view of the molecule is displayed in Figure 4, while data collection and refinement parameters are given in Table 3 and selected bond distances and angles are given in Table 4. The disorder typical for the  $(^tBu_3SiN=)_2(^tBu_3SiNH)W$  fragment is less evident in 1-CH=C=CH<sub>2</sub> as one  $W-N$  distance is statistically shorter (1.782(4) Å) than the other two (1.850(4), 1.860(4) Å). The short distance is reasonable for a tungsten imide,<sup>32,33,44</sup> and the remaining two distances may reflect an imide/amide average. The  $W-N-Si$  angle for the imide (162.6(3)°) is greater than that of the others (157.3(2), 157.4(3)°), but these angles are known to not necessarily correlate with an imide vs an amide. The core  $N-W-N$  and  $N-W-C$  angles average 114.3(28) and 104.1(19)°, respectively. The  $d(WC)$  value of 2.155(6) Å



**Figure 4.** Molecular view of  $(^t\text{Bu}_3\text{SiN}=\text{})_2(^t\text{Bu}_3\text{SiNH})\text{WCH}=\text{C}=\text{CH}_2$  ( $1\text{-CH}=\text{C}=\text{CH}_2$ ).

is roughly the same as that of  $1\text{-CH}_3$  but slightly shorter than that of the methylcyclopropyl derivative, and the allene unit is almost linear ( $\angle\text{CCC} = 178.0(10)^\circ$ ), with  $\text{CH}=\text{C}$  and  $\text{C}=\text{CH}_2$  distances of 1.183(8) and 1.320(11) Å, respectively.

**Trimethylsilyl Bromide.** The question of whether the “alkane intermediate” approach could be extended to other elements was only broached through the addition of  $\text{Me}_3\text{SiBr}$  to  $[(^t\text{Bu}_3\text{SiN}=\text{})_3\text{WH}]K$  ( $2\text{-H-K}$ ). In less than 1 h in  $\text{C}_6\text{D}_6$ , 95%  $(^t\text{Bu}_3\text{SiN}=\text{})_2(^t\text{Bu}_3\text{SiNH})\text{WSiMe}_3$  ( $1\text{-SiMe}_3$ ) was produced with 5%  $(^t\text{Bu}_3\text{SiN}=\text{})_2(^t\text{Bu}_3\text{SiNH})\text{WBr}$  ( $1\text{-Br}$ ) as a byproduct, as eq 5 indicates. Hydride delivery to the substrate, followed by



$\text{SiH}$  activation from the putative  $(^t\text{Bu}_3\text{SiN}=\text{})_3\text{W}(\text{HSiMe}_3)$  ( $2\text{-HSiMe}_3$ ) intermediate, is a logical path to  $1\text{-SiMe}_3$ .

## DISCUSSION

**General Mechanism.** Illustrations accompanying the preceding results sections have been predicated on the generation of hydrocarbon complex intermediates in the reactions of  $[(^t\text{Bu}_3\text{SiN}=\text{})_3\text{WH}]M$  ( $2\text{-H-M}$ ) with hydrocarbyl halides. Extrapolating from the modest kinetics treatment of  $2\text{-H-K}$  and  $\text{MeX}$ , the general reaction is best considered first order in  $2\text{-H-M}$  and first order in  $\text{RX}$  (Scheme 4, Table 2). The reduction step ( $\text{RX} + \text{MH} \rightarrow \text{RH} + \text{MX}$ ) can be construed as possessing hydride or electron transfer (eT) character, as the rates of  $\text{MeX}$  reduction ( $k(\text{I}^-) \approx k(\text{Br}^-) > k(\text{Cl}^-)$ ) are not particularly informative.

Scheme 13 illustrates the *single intermediate mechanism* whereby the three standard products,  $(^t\text{Bu}_3\text{SiN}=\text{})_2(^t\text{Bu}_3\text{SiNH})\text{WR}$  ( $1\text{-R}$ ),  $[(^t\text{Bu}_3\text{SiN}=\text{})_3\text{WX}]M$  ( $2\text{-X-M}$ ), and those derived from solvent,  $(^t\text{Bu}_3\text{SiN}=\text{})_2(^t\text{Bu}_3\text{SiND})\text{WC}_6\text{D}_5$  ( $1\text{-ND-C}_6\text{D}_5$ , solvent =  $\text{C}_6\text{D}_6$ ) or  $(^t\text{Bu}_3\text{SiN}=\text{})_3\text{WL}$  ( $2\text{-L}$ ,  $\text{L} = \text{OEt}_2$ , THF, etc.), are

produced upon breakup of a single intermediate,  $I$ . While this mechanism cannot be disproved, the various trials in Schemes 2 and 3 show that variation in solvent at  $60^\circ\text{C}$ , e.g.,  $\text{Et}_2\text{O}$  vs  $\text{C}_6\text{D}_6$ , with  $\text{CD}_3\text{I}$  as substrate does not change the ratio of  $(^t\text{Bu}_3\text{SiN}=\text{})_2(^t\text{Bu}_3\text{SiNH})\text{W}(\text{CD}_3/\text{CHD}_2)$  ( $1\text{-CD}_3/1\text{-ND-CHD}_2$ ) to  $1\text{-ND-C}_6\text{D}_5$  or  $2\text{-OEt}_2$ . If the solvent were intimately involved in an intermediate such as  $I$ , significant deviations would be expected.

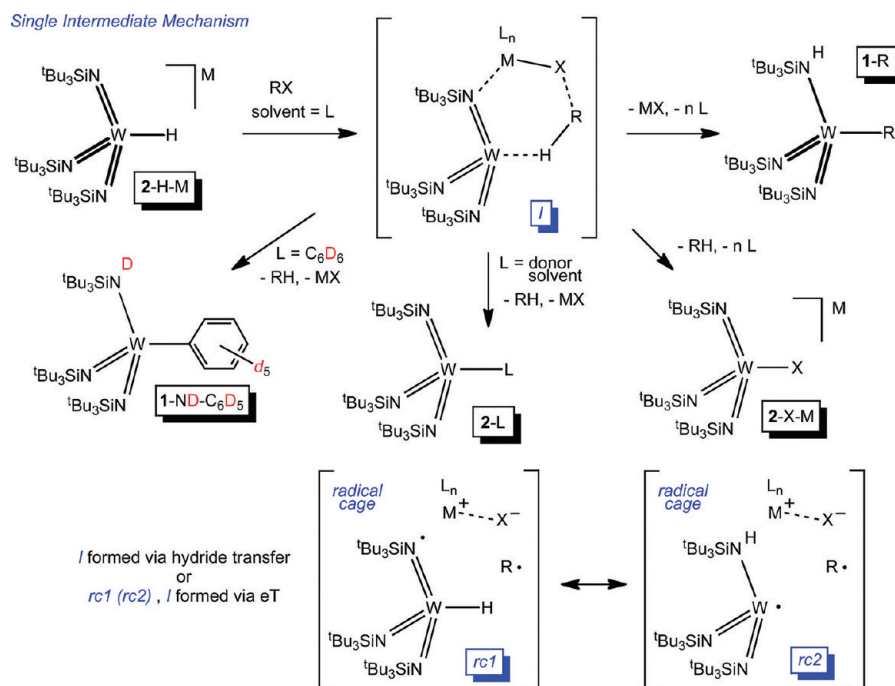
The ratio  $\{1\text{-Me} + 1\text{-ND-C}_6\text{D}_5\}/2\text{-I-K}$  does change as a function of solvent (Schemes 2–4) but does not change as  $\text{X}$  is varied in  $\text{CH}_3\text{X}$ . The former is consistent with intermediate  $I$  in Scheme 13 but is generally consistent with alternative processes, while the latter suggests that the transition state regarding reduction, either a hydride delivery or eT step, is early in a reaction coordinate whose  $\Delta G^\circ$  value is likely to be substantially favorable. Hydride delivery is implicated by intermediate  $I$ , yet it is conceivable that electron transfer to give products within a radical cage is also reasonable, provided the lifetime of  $\text{R}^\bullet$  is short compared to the time scale of rearrangement of radicals derived from radical clocks  $^t\text{PrCH}_2\text{Br}$  and 5-hexenyl bromide. Note that cage collapse of either  $rc1$  or  $rc2$  in Scheme 13 to intermediate  $I$  or to products  $1\text{-R}$  or  $\text{RH}$  via hydrogen atom abstraction (HAT)<sup>45,46</sup> provides a plausible alternative to hydride transfer, albeit on the appropriate time scale.

Scheme 14 illustrates the *double intermediate mechanism* used in describing the majority of the product distributions in Schemes 2–12. In this mechanism, the putative intermediate  $I$  degrades into  $[(^t\text{Bu}_3\text{SiN}=\text{})_3\text{WX}]M$  ( $2\text{-X-M}$ ) via loss of  $\text{RH}$  or an alkane complex intermediate,  $(^t\text{Bu}_3\text{SiN}=\text{})_3\text{W}(\text{RH})$  ( $2\text{-RH}$ ), and  $\text{MX}$ . Conversion of the latter into  $(^t\text{Bu}_3\text{SiN}=\text{})_2(^t\text{Bu}_3\text{SiNH})\text{WR}$  ( $1\text{-R}$ ) and  $(^t\text{Bu}_3\text{SiN}=\text{})_2(^t\text{Bu}_3\text{SiND})\text{WC}_6\text{D}_5$  ( $1\text{-ND-C}_6\text{D}_5$ , solvent =  $\text{C}_6\text{D}_6$ ) or  $(^t\text{Bu}_3\text{SiN}=\text{})_3\text{WL}$  ( $\text{L} = \text{donor solvent}$ ) upon loss of  $\text{RH}$  completes the scheme. It is also possible that  $I$  is a transition state that partitions to  $2\text{-X-M}$  and  $2\text{-RH}$ . Variants of intermediate  $I$  based on eT processes shown in Scheme 13 can also apply. Intermediate  $2\text{-RH}$  is likely to swiftly equilibrate with other bound forms of the alkane, i.e.,  $(^t\text{Bu}_3\text{SiN}=\text{})_3\text{W}(\text{R}^\bullet\text{H})$  ( $2\text{-R}^\bullet\text{H}$ ), such that previously established CH bond selectivities apply.<sup>20,23,38</sup> The alkane complex intermediate is supported by calculations,<sup>15–18</sup> is fully consistent with  $1,2\text{-RH}$  addition reactions observed for other imido compounds,<sup>20–28,38</sup> fits the observed changes in product ratios, etc.

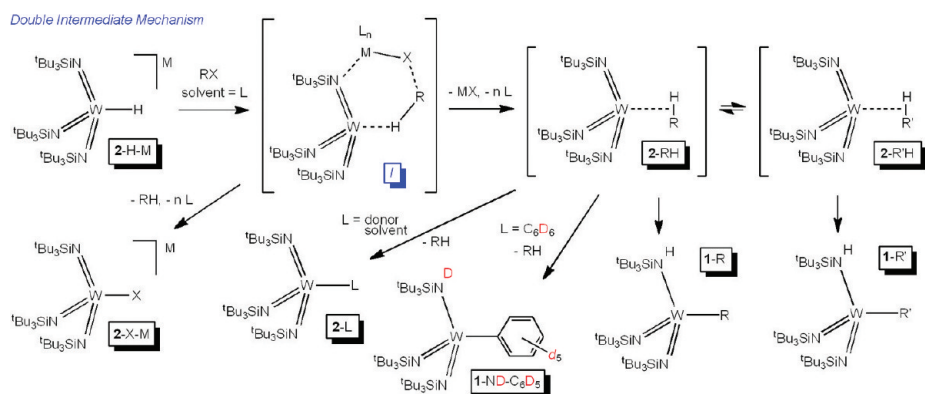
**Kinetic Isotope Effects.** The phenomenological KIEs determined for  $[(^t\text{Bu}_3\text{SiN}=\text{})_3\text{WH}]K$  ( $2\text{-H-K}$ ) plus  $\text{CD}_3\text{I}$  can be used to test the consistency of the *double intermediate mechanism* via scrutiny of the  $[1\text{-Me}]/[1\text{-ND-C}_6\text{D}_5]$  ratio vs the  $([1\text{-CD}_3] + [1\text{-ND-CHD}_2])/[1\text{-ND-C}_6\text{D}_5]$  ratio, as Scheme 15 indicates.<sup>34</sup> In the analysis, factors affecting the ratios have been kept simple. For example, since the structure of  $(^t\text{Bu}_3\text{SiN}=\text{})_3\text{W}(\text{CHD}_3)$  ( $2\text{-CHD}_3$ ) is unknown, i.e.,  $\eta\text{-CHD}_3$ ,  $\eta^2\text{-CHD}_3$ , or  $\eta^3\text{-CHD}_3$ , it is treated as a single entity, because any further complication could not be untangled with the limited data at hand.<sup>7</sup> Only the  $\text{CD}_3$  isotopologue of methyl iodide was examined; hence, secondary isotope effects cannot be teased out of the data. The analysis thus uses two KIEs: the phenomenological  $k_{\text{H}}/k_{\text{D}}$  ( $z_{\text{a}}$ ) accorded activation of the CH of bound  $\text{CHD}_3$  relative to  $1,2\text{-CD}$ -addition<sup>21,24,28</sup> and a  $z_{\text{s}}$  pertaining to the dissociation of  $\text{CH}_4$  vs  $\text{CHD}_3$ , a value that reflects their relative binding.<sup>7,49</sup>

As Scheme 15 indicates, while the  $z_{\text{a}}$  value of 9.6 is sufficient to explain the change in ratios upon deuteration with respect to

Scheme 13



Scheme 14



experimental error, solving for  $z_s$  affords a value  $<1$ , consistent with weaker binding of  $\text{CHD}_3$ . Weaker binding of deuterated methanes is due to greater attenuation of the CD bond strength when deuterium is in a bridging position: i.e.,  $\text{W}(\mu\text{-D})\text{C}$ . The subtly greater weakening of a CD bond vs the corresponding CH bond of bound  $\text{CH}_4$  is enough to bias the binding such that  $\text{CHD}_3$  is more readily lost: hence, the  $z_s$  value of 0.94 obtained from the analysis.<sup>7,49</sup> The change in ratios leading toward more solvent activation in the deuterated case is thereby ascribed to two factors: (1) 1,2-CD addition is slower by a factor of 9.6, hence, loss of methane becomes more competitive with activation and (2) loss of  $\text{CHD}_3$  from 2- $\text{CHD}_3$  occurs slightly more readily than  $\text{CH}_4$  from 2- $\text{CH}_4$ ,<sup>7</sup> leading to slightly more solvent activation.<sup>34</sup>

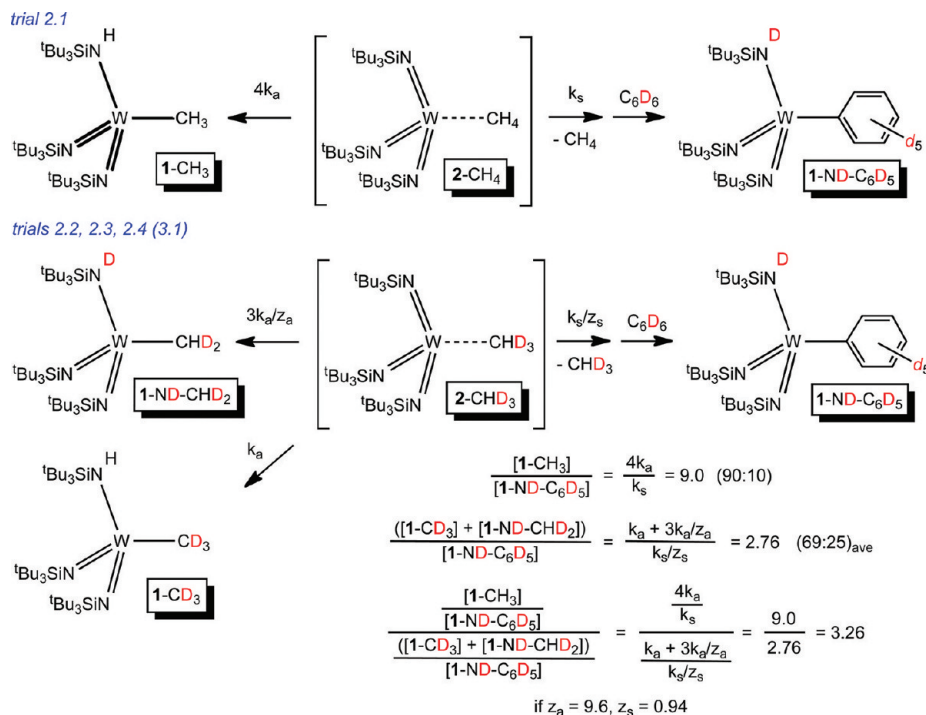
Since the data acquired in the investigation of methane activation are limited, corroboration of the KIE arguments above was sought for the case of  $\text{CH}_3\text{CH}_2\text{I}$  vs  $\text{CD}_3\text{CH}_2\text{I}$ , and this is illustrated in Scheme 16. In this analysis, the assumptions delineated above were again applied, with a single KIE that describes 1,2-CH vs 1,2-CD addition to the imide linkage ( $k_{\text{H}}/k_{\text{D}} = z_a$ ) to form  $(\text{tBu}_3\text{SiN}=\text{})_2(\text{tBu}_3\text{SiNH})\text{WCH}_2\text{CD}_3$  (1-

$\text{ND-CD}_2\text{CH}_3$ ) and  $(\text{tBu}_3\text{SiN}=\text{})_2(\text{tBu}_3\text{SiND})\text{WCD}_2\text{CH}_3$  (1-ND- $\text{CD}_2\text{CH}_3$ ) and a single KIE describing loss of ethane from  $(\text{tBu}_3\text{SiN}=\text{})_3\text{W}(\text{CH}_3\text{CH}_3)$  (2- $\text{CH}_3\text{CH}_3$ ) vs  $(\text{tBu}_3\text{SiN}=\text{})_3\text{W}(\text{CH}_3\text{CD}_3)$  (2- $\text{CH}_3\text{CD}_3$ ) ( $k_{\text{H}}/k_{\text{D}} = z_s$ ). The ratio of ratios was obtained from the product breakdown in trials 5.1 and 5.2, and a  $z_a$  value of 7.9 yielded a  $z_s$  value  $<1$ . Again, the change in ratios can be explained solely by the slowdown in 1,2-CD addition from 2- $\text{CH}_3\text{CD}_3$  within the constraints of experimental error, but the calculated addition of  $z_s = 0.89$  is consistent with weaker binding of  $\text{CH}_3\text{CD}_3$  as a contributing factor.<sup>7</sup>

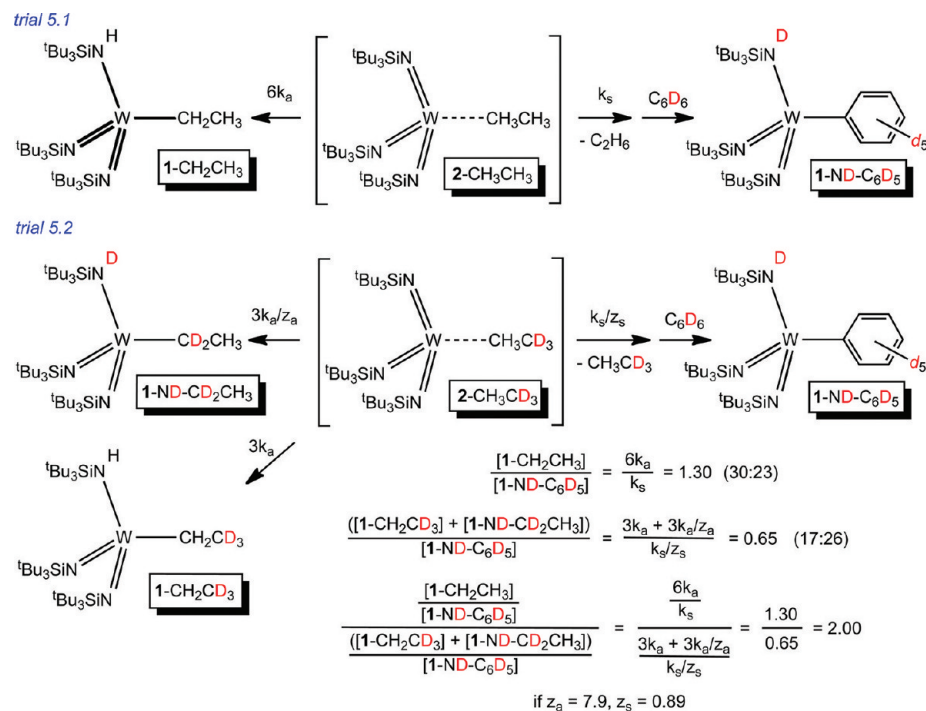
**Radical Paths.** Since the two radical clocks employed in this study failed to elicit evidence of radical paths, methyl and primary halides are considered reduced by hydride transfer or by radical processes swift enough to bypass the clock rearrangements. In the cases of secondary and tertiary halides and ethyl, evidence for radical processes exists in the product distributions.<sup>47,48</sup> Consider the standard radical processes summarized in Scheme 17, where the initial electron transfer (II) from  $[(\text{tBu}_3\text{SiN}=\text{})_3\text{WH}]\text{M}$  (2-H-M) plus  $\text{RX}$  yields  $\text{R}^\bullet$  and a metallaradical. A subsequent halide abstraction by the



Scheme 15



Scheme 16



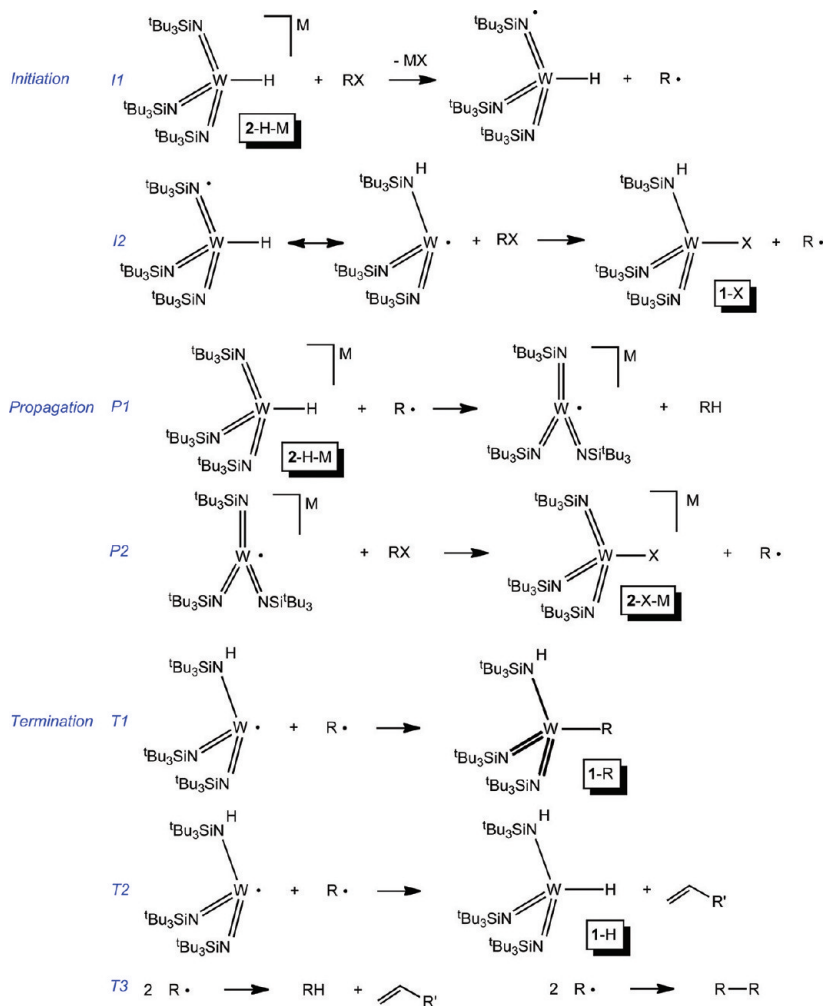
metalloradical (*I2*) can generate another 1 equiv of  $R^\bullet$  and  $(^t\text{Bu}_3\text{SiN}=\text{})_2(^t\text{Bu}_3\text{SiNH})\text{WX}$  (**1-X**).

Scheme 7 shows that **1-X** is a prominent product for *tert*-butyl and neopentyl halides, and for the latter substrate it increases in the order  $\text{X} = \text{Cl} < \text{Br} < \text{I}$ , consistent with halide abstraction. Even in the cases of EtBr and EtI, significant amounts of **1-X** ( $\text{X} = \text{Br}, \text{I}$ ) are generated. For the hindered primary, secondary, and tertiary substrates in Scheme 7, the amounts of **2-X-K** and **1-X** encompass  $\geq 69\%$  of the products.

For the *tert*-butyl cases, 0–2% of **2-X-K** is produced, and the  $\sim 1/1$  ratio of isobutylene and isobutene products suggests that propagation steps (*P1*, *P2*) leading to **2-X-K** are not competitive. In contrast, the less hindered neopentyl radical appears likely to abstract a hydrogen atom from **2-H-K** in a propagation sequence, leading to substantial amounts of **2-X-K**, and in the case of  $^{\text{neo}}\text{PeCl}$  and **2-H-Na** (trial 7.3), the 100% formation of **2-Cl-Na** is consistent with an efficient radical chain. Likewise, in the case of  $^i\text{PrI}$  reduction, a greater amount



Scheme 17



of 2-I-K than of 1-I was produced, and all three organic termination products expected for isopropyl radical—propane, propene, and 2,3-dimethylbutane—are observed. In the isobutyl (trial 7.1) and cyclohexylmethyl bromide (trial 7.2) substrates, the amount of RH formed is greater than that of the unsaturated organics; thus, chain processes may account for the majority of RH. While it was difficult to determine whether the product ratios were constant or changing during the course of reduction,<sup>48</sup> there is enough evidence to conclude that radical processes are competent for substrates that are hindered. The situation is very similar to observations of oxidative additions of RX to reduced metal centers, where  $\text{S}_{\text{N}}2$  vs radical mechanisms are extremely sensitive to the size and type of R.

**Selectivities.** Selectivities for the type of CH bond activated via the intermediate alkane (arene) species  $(t\text{Bu}_3\text{SiN})_3\text{W}(\text{RH})$  (2-RH) follow previously established trends.<sup>20,23,38–40</sup> For example, in instances where  $\text{sp}^3\text{-CH}$  vs  $\text{sp}^2\text{-CH}$  bond activations are competing, the product was invariably derived from the latter. In the related cases of 2-RH (RH = toluene, xylene, mesitylene),<sup>39,40</sup> the product ratios at 23 °C could be used to assess the relative  $\Delta\Delta G^\ddagger$  value for arene activation at sites with no *o*-Me ( $A_0$ ), one *o*-Me ( $A_1$ ), and two *o*-Me ( $A_2$ ) groups versus benzylic activation (B) and arene loss (E). On comparison of the product ratios in Scheme 10 and correction for statistics, the following relative activation order was ascertained:  $A_0$  (both para and meta activation of toluene,

i.e., [1-*p*-tol] and [1-*m*-tol]) is lowest;  $A_1$ ,  $\Delta\Delta G^\ddagger > 2.5$  kcal/mol relative to  $A_0$ ; B,  $\Delta\Delta G^\ddagger > 2.7$  relative to  $A_0$ ,  $\Delta\Delta G^\ddagger = 1.3$  kcal/mol relative to  $A_1$ ; E,  $\Delta\Delta G^\ddagger = 0.75$  kcal/mol relative to B;  $A_2$ ,  $\Delta\Delta G^\ddagger > 2.1$  kcal/mol relative to B. Activation of toluene at the para and meta positions is roughly favored over ortho activation by  $>2.5$  kcal/mol and over benzylic activation by  $>3.8$  kcal/mol, while arene activation between two methyl groups is disfavored by  $>5.9$  kcal/mol. The relative selectivities appear general to oxidative addition reactions<sup>39,40</sup> and 1,2-RH additions to imido units.

## CONCLUSIONS

In cases of unhindered  $\text{sp}^3$  alkyl halides, reduction of RX by  $[(t\text{Bu}_3\text{SiN})_3\text{WH}]\text{M}$  (2-H-M) proceeds to afford  $[(t\text{Bu}_3\text{SiN})_3\text{WX}]\text{M}$  (2-X-M) and RH or loss of MX and products derived from an alkane or arene complex intermediate,  $(t\text{Bu}_3\text{SiN})_3\text{W}(\text{RH})$  (2-RH). For hindered  $\text{sp}^3$  substrates, radical paths change the nature of the product distribution toward halide products. Through exhaustive studies of 2-H-M plus RX, a consistent pattern has emerged that dovetails with previous studies regarding the 1,2-RH elimination from  $\text{XY}(t\text{Bu}_3\text{SiNH})\text{MR}$  and 1,2-RH addition to transient  $\text{XY}(t\text{Bu}_3\text{SiN})\text{M}$ .

The indirect observation of various  $(t\text{Bu}_3\text{SiN})_3\text{W}(\text{RH})$  (2-RH) suggests that intermediates  $(t\text{Bu}_3\text{SiO})_2(t\text{Bu}_3\text{SiN})\text{Ti}(\text{RH})$ ,<sup>20,21</sup>  $(t\text{Bu}_3\text{SiNH})_2(t\text{Bu}_3\text{SiN})\text{Ti}(\text{RH})$ ,<sup>22</sup>

(<sup>t</sup>Bu<sub>3</sub>SiNH)<sub>2</sub>(<sup>t</sup>Bu<sub>3</sub>SiN=)Zr(RH),<sup>23,24</sup> (<sup>t</sup>Bu<sub>3</sub>SiNH)(<sup>t</sup>Bu<sub>3</sub>SiN=)<sub>2</sub>V(RH),<sup>25,26</sup> and (<sup>t</sup>Bu<sub>3</sub>SiNH)(<sup>t</sup>Bu<sub>3</sub>SiN=)<sub>2</sub>Ta(RH)<sup>27</sup> are likely to be operable in these related systems. In low-valent late-transition-metal species, L<sub>n</sub>M(RH) reactions also precede C–H bond activation to give L<sub>n</sub>M(H)R, and activation selectivities are determined by RH binding.<sup>12,39,49</sup> In contrast, 1,2-RH addition is the selectivity-determining event for the titanium, zirconium, vanadium, and tantalum d<sup>0</sup> imido complexes. The standard free energy for 1,2-RH addition to putative (<sup>t</sup>Bu<sub>3</sub>SiN=)<sub>3</sub>W (2) is very favorable; thus, it is competitive with alkane loss in this investigation. Alkane loss from 2-RH is noted by solvent activation to give (<sup>t</sup>Bu<sub>3</sub>SiN=)<sub>2</sub>(<sup>t</sup>Bu<sub>3</sub>SiND)WC<sub>6</sub>D<sub>5</sub> (1-ND-C<sub>6</sub>D<sub>5</sub>, solvent = C<sub>6</sub>D<sub>6</sub>). Phenomenological KIEs obtained via substrates CD<sub>3</sub>I and CD<sub>3</sub>CH<sub>2</sub>I are in line with those obtained for CHD<sub>3</sub> and CH<sub>3</sub>CD<sub>3</sub> activations by putative (<sup>t</sup>Bu<sub>3</sub>SiO)<sub>2</sub>(<sup>t</sup>Bu<sub>3</sub>SiN=)Ti and related imido complexes,<sup>21,24</sup> providing additional evidence for the intermediacy of 2-RH. In cases where 2-RH contains different CH bonds, the selectivity of bond activation follows previously established selectivity patterns;<sup>20,23,38</sup> hence, it is likely that a rapid equilibrium is established between various binding conformations subsequent to generation of the initial 2-RH. On the basis of this work, previous KIEs determined for 1,2-RH/D addition to (<sup>t</sup>Bu<sub>3</sub>SiO)<sub>2</sub>(<sup>t</sup>Bu<sub>3</sub>SiN=)Ti and related imido species are likely to be comprised of binding and 1,2-addition events.<sup>21,24</sup>

## EXPERIMENTAL SECTION

**General Considerations.** All manipulations were performed using either glovebox or high-vacuum-line techniques. All glassware was oven-dried. THF and ether were distilled under nitrogen from purple sodium benzophenone ketyl and vacuum-transferred from the same prior to use. Hydrocarbon solvents were treated in the same manner with the addition of 1–2 mL/L tetraglyme. Benzene-*d*<sub>6</sub> and toluene-*d*<sub>8</sub> were dried over sodium, vacuum-transferred and stored over activated 4 Å molecular sieves. THF-*d*<sub>8</sub> was dried over sodium and vacuum-transferred from sodium benzophenone ketyl prior to use. All glassware was base-washed and oven-dried. NMR tubes for sealed-tube experiments were flame-dried under dynamic vacuum prior to use. Alkyl and aryl halides and other organic reagents were obtained from Aldrich Chemical except for CD<sub>3</sub>CH<sub>2</sub>I (Cambridge Isotope Laboratories) and 3,5-dimethylbenzyl bromide (Johnson Matthey). Volatile alkyl halides were degassed, distilled, and dried over activated 4 Å molecular sieves, except for bromomethylcyclopropane, which decomposed when exposed to sieves. Less volatile substrates were subjected to degassing and used as received. The compounds (<sup>t</sup>Bu<sub>3</sub>SiNH)(<sup>t</sup>Bu<sub>3</sub>SiN=)<sub>2</sub>WX (1-X; X = Cl, Br, I), (<sup>t</sup>Bu<sub>3</sub>SiNH)(<sup>t</sup>Bu<sub>3</sub>SiN=)<sub>2</sub>WR (1-R; R = H, Me, Et, <sup>n</sup>Pr, Ph, C<sub>6</sub>H<sub>4</sub>-3-Me, C<sub>6</sub>H<sub>4</sub>-4-Me, Bn), [(<sup>t</sup>Bu<sub>3</sub>SiN=)<sub>3</sub>WH]M (2-H-M; M = Na, K), [(<sup>t</sup>Bu<sub>3</sub>SiN=)<sub>3</sub>WX]K (2-X-K; X = Cl, Br, I), and [(<sup>t</sup>Bu<sub>3</sub>SiN=)<sub>3</sub>WX]Na (2-X-Na; X = Cl, Br) were either prepared or identified in an accompanying paper.<sup>30</sup>

<sup>1</sup>H, <sup>13</sup>C{<sup>1</sup>H}, and <sup>2</sup>H{<sup>1</sup>H} NMR spectra were obtained using Varian XL-200, XL-400, and Unity-500 spectrometers. Chemical shifts are reported relative to benzene-*d*<sub>6</sub> (<sup>1</sup>H, δ 7.15; <sup>13</sup>C, δ 128.00) or THF-*d*<sub>8</sub> (<sup>1</sup>H, δ 3.58; <sup>13</sup>C, δ 67.57). Infrared spectra were recorded on a Nicolet Impact 410 spectrophotometer interfaced to a Gateway PC. Combustion analyses were conducted by Oneida Research Services, Whitesboro, NY, or Robertson Microlit Laboratories, Madison, NJ.

**Procedures.** 1. [(<sup>t</sup>Bu<sub>3</sub>SiN=)<sub>3</sub>WH]K (2-H-K) + CD<sub>3</sub>I (Excess).

(a). *General Considerations.* In a small glass bomb was loaded 2-H-K, followed by evacuation and distillation of the appropriate solvent. Roughly 10 equiv of CD<sub>3</sub>I was vacuum-transferred and the bomb placed in a heated oil bath. At the completion of the reaction, the volatiles were removed in vacuo and the resulting mixture was analyzed by NMR spectroscopy. The ratio of 1-ND-CD<sub>2</sub>H to 1-CD<sub>3</sub> was obtained by assuming the <sup>2</sup>H{<sup>1</sup>H} resonance at δ 1.41

corresponded to the resonances of the CD<sub>2</sub>H of 1-ND-CD<sub>2</sub>H and the CD<sub>3</sub> of 1-CD<sub>3</sub>, while the resonance at δ 6.60 corresponds to the ND of 1-ND-CD<sub>2</sub>H.

(b). *C<sub>6</sub>H<sub>6</sub> Solvent.* 2-H-K (125 mg, 0.145 mmol) in 5 mL of benzene and 469 Torr of CD<sub>3</sub>I (50.4 mL gas bulb, 1.28 mmol, 9 equiv) were stirred for 10 h at 60 °C. The products were assayed by NMR spectroscopy (Scheme 2), and a <sup>2</sup>H{<sup>1</sup>H} NMR spectrum revealed the ratio of 1-ND-CD<sub>2</sub>H to 1-CD<sub>3</sub> to be 3.2(2).

(c). *Et<sub>2</sub>O Solvent.* 2-H-K (200 mg, 243 mmol) in 10 mL of Et<sub>2</sub>O and 185 Torr of CD<sub>3</sub>I (0.266 L gas bulb, 2.68 mmol, 11.5 equiv) were stirred for 11 h at 60 °C. The products were assayed by NMR spectroscopy (Scheme 3), and a <sup>2</sup>H{<sup>1</sup>H} NMR spectrum revealed the ratio of 1-ND-CD<sub>2</sub>H to 1-CD<sub>3</sub> to be 3.3(2). A sample (10 mg) of the crude reaction mixture was taken up in C<sub>6</sub>D<sub>6</sub>, sealed in an NMR tube, and subjected to thermolysis at 150 °C. 2-OEt<sub>2</sub> was shown to convert to 1-ND-C<sub>6</sub>D<sub>5</sub> with *t*<sub>1/2</sub> < 10 h (assume unimolecular; Δ*G*<sup>‡</sup> ≈ 34 kcal/mol).

(d). *THF Solvent.* 2-H-K (0.165 g, 0.191 mmol) in 10 mL of THF and 132 Torr of CD<sub>3</sub>I (0.266 L gas bulb, 1.91 mmol, 10 equiv) were stirred for 75 min at 100 °C. The products were assayed by NMR spectroscopy (Scheme 3), and a <sup>2</sup>H{<sup>1</sup>H} NMR spectrum revealed the ratio of 1-ND-CD<sub>2</sub>H to 1-CD<sub>3</sub> to be 3.9(2). A sample (10 mg) of the crude reaction mixture was taken up in C<sub>6</sub>D<sub>6</sub>, sealed in an NMR tube, and subjected to thermolysis at 150 °C. 2-THF slowly converted to 1-ND-C<sub>6</sub>D<sub>5</sub> with *t*<sub>1/2</sub> < 10 h (assume unimolecular; Δ*G*<sup>‡</sup> ≈ 37 kcal/mol).

2. (<sup>t</sup>Bu<sub>3</sub>SiNH)(<sup>t</sup>Bu<sub>3</sub>SiN=)<sub>2</sub>WR (1-E/Z-CH=CHMe). (a). *Preparation.* In a 100 mL glass bomb shielded from ambient light containing 2-H-K (640 mg, 0.740 mmol) was transferred 30 mL of benzene followed by 512 Torr of allyl iodide by vacuum transfer (266 mL gas bulb, 7.40 mmol, 10 equiv). The vessel was placed in a 60 °C bath for 8.5 h, and the initially colorless solution turned light yellow. After the mixture was cooled to 23 °C and volatiles were removed, the remaining solid was dissolved in 5 mL of hexanes, the solution was filtered, and the solvent was replaced with THF. Subsequent cooling to –78 °C gave a milky suspension which was collected as a light yellow powder by filtration (180 mg, 28%). The <sup>1</sup>H NMR spectrum of the crude reaction mixture revealed the ratio of *Z*- to *E*-1-C(H)=C(H)Me to be 33(2). A corresponding NMR tube scale reaction showed quantitative conversion of 2-H-K to tungsten vinyl products. IR (Nujol, cm<sup>–1</sup>): 3249 (m, NH), 1578 (m, C=C), 1468 (s), 1386 (s), 1364 (m), 1130 (s), 1055 (s), 1040 (s), 1009 (s), 971 (m), 934 (m), 846 (s), 819 (s), 643 (m), 621 (s), 582 (s). Anal. Calcd for C<sub>39</sub>H<sub>87</sub>N<sub>3</sub>Si<sub>3</sub>W: C, 54.08; H, 10.12; N, 4.85. Found: C, 53.71; H, 9.99; N, 4.67.

(b). *Thermolysis and Photolysis.* Samples of 1-CH=CHMe were loaded into two NMR tubes and dissolved in benzene-*d*<sub>6</sub> and the tubes sealed. One was shielded from light and heated to 150 °C for 7 days; analysis by <sup>1</sup>H NMR spectroscopy indicated no evidence of isomerization. The second sample was subjected to a 20 W laboratory fluorescent light for 12 h at 23 °C, affording a photostationary *Z* to *E* ratio of 1.21(3)/1. Subsequent thermolysis in the dark at 150 °C for 7 days showed no deviation from this ratio.

3. (<sup>t</sup>Bu<sub>3</sub>SiNH)(<sup>t</sup>Bu<sub>3</sub>SiN=)<sub>2</sub>W(6/7-Me-2-nap) (1-6/7-Me-2-nap). In a glass bomb reactor, 2-(bromomethyl)naphthalene and 2-H-K were combined and 30 mL of benzene was added at –78 °C via distillation. The mixture was heated to 60 °C for 11 h. After removal of volatiles, the resulting solids were taken up in hexanes, and the solution was filtered, concentrated, and cooled to –78 °C. 1-6/7-Me-2-nap was collected as a light yellow solid by filtration (152 mg, 26%) and assayed by <sup>1</sup>H NMR spectroscopy (Scheme 10). Anal. Calcd for C<sub>47</sub>H<sub>91</sub>N<sub>3</sub>Si<sub>3</sub>W: C, 58.42; H, 8.45; N, 4.35. Found: C, 58.52; H, 8.82; N, 4.13.

4. (<sup>t</sup>Bu<sub>3</sub>SiNH)(<sup>t</sup>Bu<sub>3</sub>SiN=)<sub>2</sub>WCH=CH<sup>n</sup>Bu (1-CH=CH<sup>n</sup>Bu). A small bomb reactor containing 2-H-K (0.920 g, 1.06 mmol) and 20 mL of benzene was cooled to –78 °C, and 6-bromo-1-hexene (1.2 mL, 8.5 equiv) was admitted by vacuum transfer. The colorless solution was heated at 100 °C for 24 h to give a yellow solution with a precipitate. After removal of the volatiles the residue was subject to sublimation at 80 °C and 10<sup>–4</sup> Torr to remove unreacted substrate. The remaining

material was taken up in hexanes, filtered, and passed through a basic alumina column (ICN, activity grade I, for removal of 2-Br-K). The hexanes were removed and replaced by bis(trimethylsilyl) ether, and the resulting solution was cooled to  $-45\text{ }^{\circ}\text{C}$ , yielding 1-C(H)=C(H)<sup>t</sup>Bu, which was collected as a yellow powder by filtration (240 mg, 25%).  $^1\text{H}$  NMR spectral analysis showed the Z to E ratio to be 7.1/1 in addition to a small amount of 1-Br (<10%). IR (Nujol,  $\text{cm}^{-1}$ ): 3243 (w, NH), 1579 (w, C=C), 1467 (s), 1386 (s), 1365 (m), 1138 (s), 1045 (s), 1009 (s), 934 (m), 848 (s), 819 (s), 621 (s), 581 (s). Anal. Calcd for  $\text{C}_{42}\text{H}_{93}\text{N}_3\text{Si}_3\text{W}$ : C, 55.54; H, 10.32; N, 4.63. Found: C, 54.57; H, 9.90; N, 4.52.

5. ( $^t\text{Bu}_3\text{SiNH}$ )( $^t\text{Bu}_3\text{SiN}=\text{}$ ) $_2\text{W}^{\text{t}}\text{PrMe}$  (1- $^t\text{PrMe}$ ). (a). *Preparation.* A small bomb reactor containing 2-H-K (0.860 g, 0.995 mmol) and 25 mL of benzene was cooled to  $-78\text{ }^{\circ}\text{C}$ , and  $^t\text{PrCH}_2\text{Br}$  (1.0 g, 7.4 equiv) was admitted by vacuum transfer. The colorless solution was heated to  $100\text{ }^{\circ}\text{C}$  for 6 h, giving a light pink solution with a precipitate. After removal of the volatiles the residue was subject to sublimation at  $80\text{ }^{\circ}\text{C}$  at  $10^{-4}$  Torr. The remaining material was taken up in hexanes, filtered, and passed through a basic alumina column (ICN, activity grade I). The hexanes were removed and replaced by bis(trimethylsilyl) ether, and the resulting solution was cooled to  $-45\text{ }^{\circ}\text{C}$ , yielding 1- $^t\text{PrMe}$ , which was collected as an off-white powder by filtration (454 mg, 52%). A  $^1\text{H}$ - $^1\text{H}$  E.COSY experiment (Varian Unity 500 spectrometer; 500.518 MHz) was conducted, and 8192 complex points in F2 and 150 complex points in F1 were acquired. Zero filling in both dimensions resulted in a final spectrum of  $8192 \times 512$  real data points. The digital resolution was 0.5 Hz/pt in the F2 dimension and 8.0 Hz/pt in the F1 dimension. A total of 32 transients were collected for each FID using a relaxation delay of 1.5 s. Phase-sensitive acquisition was achieved by the hypercomplex method of States, Haberkorn, and Ruben.<sup>50</sup> IR (Nujol,  $\text{cm}^{-1}$ ): 3254 (w, NH), 1468 (s), 1385 (s), 1131 (m), 1044 (s), 1008 (s), 935 (m), 846 (s), 820 (s), 621 (s), 582 (m). Anal. Calcd for  $\text{C}_{40}\text{H}_{89}\text{N}_3\text{Si}_3\text{W}$ : C, 54.58; H, 10.19; N, 4.77. Found: C, 54.31; H, 10.35; N, 4.84.  $^1\text{H}$  NMR spectral analysis of the original reaction mixture revealed the composition to be 91% 1- $^t\text{PrMe}$  and 9% 1-C(H)=C(H)Et.

(b). *NMR Tube Scale.* 2-H-K and 10 equiv of  $^t\text{PrCH}_2\text{Br}$  were heated at  $100\text{ }^{\circ}\text{C}$  for 6 h.  $^1\text{H}$  and  $^{13}\text{C}\{^1\text{H}\}$  NMR spectral analysis indicated formation of 86% 1- $^t\text{PrMe}$ , 4% 1-C(H)=C(H)Et, 8% 2-Br-K, 2% 1-Br, and 1-butene.

6. ( $^t\text{Bu}_3\text{SiNH}$ )( $^t\text{Bu}_3\text{SiN}=\text{}$ ) $_2\text{WCH}=\text{C}=\text{CH}_2$  (1- $\text{CH}=\text{C}=\text{CH}_2$ ). (a). *Preparation.* Propargyl bromide (0.8 mL, 7.2 mmol, 12 equiv) was condensed into a glass reaction vessel containing 2-H-K (520 mg, 0.602 mmol) and 20 mL of hexanes. The reaction mixture was stirred at  $60\text{ }^{\circ}\text{C}$  for 8 h, and the colorless solution changed to light red. Following removal of all volatiles, the remaining material was taken up in hexanes, filtered, condensed to  $\sim 3\text{ mL}$ , and cooled to  $-78\text{ }^{\circ}\text{C}$ . The resulting light yellow powder was collected by filtration to yield 160 mg of 1- $\text{CH}=\text{C}=\text{CH}_2$  (31%). IR (Nujol,  $\text{cm}^{-1}$ ): 3249 (m, NH), 1915 (s, C=C=C<sub>asym</sub>), 1470 (s), 1387 (s), 1365 (s), 1143 (s), 1128 (s), 1045 (s), 1009 (s), 935 (s), 845 (s), 820 (s), 792 (m), 622 (s), 582 (s). Anal. Calcd for  $\text{C}_{39}\text{H}_{85}\text{N}_3\text{Si}_3\text{W}$ : C, 54.20; H, 9.91; N, 4.86. Found: C, 53.87; H, 9.66; N, 4.91.

(b). *NMR Tube Scale.* A corresponding NMR tube scale reaction with 0.008 g of 2-H-K ( $9.3 \times 10^{-6}$  mol) and 10 equiv of propargyl bromide was heated for 24 h at  $60\text{ }^{\circ}\text{C}$  and then assayed by NMR spectroscopy (Scheme 12).

7. ( $^t\text{Bu}_3\text{SiN}=\text{}$ ) $_2\text{W}(\kappa\text{-N},\text{C}-\text{N}(\text{Si}^t\text{Bu}_3)\text{C}(\text{Me})\text{C}(\text{Me})-)$  (3-MeCCMe). 1-Bromo-2-butyne (1.3 mL, 15 mmol, 15 equiv) was condensed into a glass reaction vessel containing 2-H-K (850 mg, 0.995 mmol) and 20 mL of hexanes. The reaction mixture was stirred at  $23\text{ }^{\circ}\text{C}$  for 24 h. The colorless solution changed to light red within 10 min and gradually became deep red. Following removal of all volatiles, the remaining material was taken up in hexanes, filtered, condensed to  $\sim 3\text{ mL}$ , and cooled to  $-78\text{ }^{\circ}\text{C}$  for 10 h. The resulting purple powder was collected by filtration to yield 320 mg (36%). Analysis by  $^1\text{H}$  NMR revealed a 6/1 ratio of 3-MeCCMe to ( $^t\text{Bu}_3\text{SiN}=\text{}$ ) $_2\text{W}(\kappa\text{-C},\eta^3\text{-C}_3\text{N-CH}_2\text{CMe}_2\text{Si}-(^t\text{Bu}_2\text{N})\text{NCMeCHMe}$ ) (4-MeCCMe). IR (Nujol,  $\text{cm}^{-1}$ ): 1478 (s, br), 1386 (s), 1363 (s), 1263 (w), 1185 (m), 1139 (s), 1116 (s), 1050 (s), 1009 (s), 987 (s), 934 (s), 845 (m), 818 (s), 715 (s), 618 (s), 581 (s).

Anal. Calcd for  $\text{C}_{40}\text{H}_{87}\text{N}_3\text{Si}_3\text{W}$  (a mixture of isomers): C, 54.70; H, 9.98; N, 4.78. Found: C, 54.51; H, 9.81; N, 4.61.

8. ( $^t\text{Bu}_3\text{SiNH}$ )( $^t\text{Bu}_3\text{SiN}=\text{}$ ) $_2\text{WSiMe}_3$  (1-SiMe<sub>3</sub>). A small flask containing 2-H-K (0.500 g, 0.580 mmol) and 25 mL of benzene was cooled to  $-78\text{ }^{\circ}\text{C}$ , and bromotrimethylsilane (8.5 equiv) was admitted by vacuum transfer. The colorless solution was stirred at  $23\text{ }^{\circ}\text{C}$  for 3 h, forming a light yellow solution with undissolved precipitate. After removal of the volatile components, the remaining material was taken up in hexanes and filtered and hexanes replaced by bis(trimethylsilyl) ether. The resulting solution was cooled to  $-78\text{ }^{\circ}\text{C}$  to give a milky suspension of 1-SiMe<sub>3</sub>, which was collected as a white powder by filtration (70 mg, 13%). IR (Nujol,  $\text{cm}^{-1}$ ): 3222 (m), 1477 (s), 1470 (s), 1385 (s), 1364 (m), 1250 (w), 1238 (m), 1127 (s), 1036 (s), 1008 (s), 934 (m), 849 (s), 830 (s), 820 (s), 737 (m), 621 (s), 579 (s). Anal. Calcd for  $\text{C}_{39}\text{H}_{91}\text{N}_3\text{Si}_4\text{W}$ : C, 52.14; H, 10.05; N, 4.68. Found: C, 52.25; H, 10.04; N, 4.69.

**NMR Tube Reactions.** Flame-dried NMR tubes sealed to 14/20 ground glass joints were charged with 2-H-K (typically 10 mg,  $1.2 \times 10^{-5}$  mol) in the drybox and removed to the vacuum line on needle valve adapters. The NMR tube was degassed, deuterated solvent was vacuum-transferred, and the volatile reagents were introduced by vacuum transfer via a calibrated gas bulb at  $-196\text{ }^{\circ}\text{C}$ . The tubes were then sealed with a torch. Solid substrates were loaded with 2-H-K followed by solvent transfer on the vacuum line and flame-sealing. All reactions were performed in  $\text{C}_6\text{D}_6$  with an excess of alkyl halide, usually  $\sim 10$  equiv. Consult the schemes and equations for product distributions determined by  $^1\text{H}$ ,  $^{13}\text{C}\{^1\text{H}\}$ , and  $^2\text{H}\{^1\text{H}\}$  NMR spectroscopy. In certain circumstances, such as conversion of the 6/1 3-MeCCMe to 4-MeCCMe mixture to 4-MeCCMe, the solids were simply added to the NMR tube in the drybox, deuterated solvent was added, and the tube was sealed under vacuum for thermolysis.

**General Kinetics Procedures.** Solutions of 2-H-M (M = Na, K) were prepared with  $\text{C}_6\text{D}_6$  in 2 mL volumetric flasks. Bis(trimethylsilyl) ether ( $\sim 0.5\text{ }\mu\text{L}$ ) was added as an internal integration standard. Three samples of 0.6 mL each were transferred to flame-dried 5 mm NMR tubes joined to 14/20 joints and attached to needle valves. The tubes were subject to three freeze-pump-thaw degas cycles followed by transfer of the  $\text{CH}_3\text{X}$  (X = Cl, Br, I) substrate via a calibrated gas bulb prior to flame-sealing under vacuum. For kinetic runs able to be completed in 3 h or less, the NMR tubes were individually placed in the NMR probe preheated to  $60.0\text{ }^{\circ}\text{C}$  and the reaction was allowed to proceed. For longer runs, the three NMR tubes were simultaneously submerged in a  $60.0\text{ }^{\circ}\text{C}$  polyethylene glycol bath with a Tamson immersion circulator. In both cases the temperature was stable to  $\pm 0.3\text{ }^{\circ}\text{C}$ . Rates of disappearance were monitored by measuring the integrated intensity of the hydride tungsten satellite at  $\delta\text{ }6.80$  in the case of both 2-H-K and 2-H-Na. Integration of the satellite was required due to the obstruction of the central resonance by the residual solvent protons. The low relative intensity of the satellites necessitated using 16 transient spectra for data collection recorded at measured time intervals. All runs were monitored for 3–4 half-lives except the slowest (Table 2). Rates and uncertainties were obtained from nonlinear, nonweighted least-squares fitting to the exponential form of the rate expression, averaged for the three NMR tubes for each run.

**Single-Crystal X-ray Diffraction Studies.** 1. ( $^t\text{Bu}_3\text{SiN}=\text{}$ ) $_2\text{W}(\kappa\text{-C},\eta^3\text{-C}_3\text{N-CH}_2\text{CMe}_2\text{Si}-(^t\text{Bu}_2\text{N})\text{NCMeCHMe}$ ) (4-MeCCMe). A colorless crystal ( $0.4 \times 0.3 \times 0.2\text{ mm}$ ) of 1- $\text{CH}_3$ , obtained by slow cooling of a hexanes solution, was mounted in a glass capillary and placed on a goniometer head on a Siemens P4 four-circle diffractometer that utilized graphite-monochromated Mo  $K\alpha$  radiation ( $\lambda = 0.71073\text{ }\text{\AA}$ ). The data were collected at  $22\text{ }^{\circ}\text{C}$  using an  $\omega$ -scan with variable speed of  $2\text{--}30^{\circ}/\text{min}$ . Preliminary diffraction data revealed a monoclinic crystal system, and a hemisphere routine was used for data collection. The data consisted of 6726 reflections, 6027 of which were symmetry independent ( $R_{\text{int}} = 0.0373$ ) and 4651 were greater than  $2\sigma(I)$ . The structure was solved by direct methods (SHELXS), completed by difference Fourier syntheses, and refined by full-matrix least-squares procedures (SHELXL).<sup>51</sup> The refinement utilized  $w^{-1} = \sigma^2(F_o^2) + (0.0288p)^2 + 2.0041p$ , where  $p =$



$(F_o^2 + 2F_c^2)/3$ . All non-hydrogen atoms were refined anisotropically, and hydrogen atoms were included at calculated positions.

2.  $(^t\text{Bu}_3\text{SiN}=\text{C})(^t\text{Bu}_3\text{SiNH})\text{W}(\text{C}(\text{CH}_3)_2\text{CHMe})$  (**1-<sup>t</sup>PrMe**). A colorless block ( $0.2 \times 0.1 \times 0.05$  mm) of **1-<sup>t</sup>PrMe**, obtained by slow evaporation of an  $\text{Et}_2\text{O}$  solution, was immersed in polyisobutylene, extracted on a glass fiber, and placed under a 173 K nitrogen stream on the goniometer head of a Siemens SMART CCD area detector system equipped with a fine-focus Mo X-ray tube ( $\lambda = 0.71073$  Å). Preliminary diffraction data revealed a triclinic crystal system, and a hemisphere routine was used for data collection. The data were processed via the Bruker SAINT program to afford 17 566 reflections, 10 170 of which were symmetry independent ( $R_{\text{int}} = 0.1330$ ) and 3161 were greater than  $2\sigma(I)$ . The data were corrected for absorption with SADABS, and the structure was solved by direct methods (SHELXS), completed by difference Fourier syntheses, and refined by full-matrix least-squares procedures (SHELXL).<sup>51</sup> The data quality was poor and the structure was initially solved in *P*1, until pairs of molecules were found to be related by an inversion center; the structure was transformed to and refined in *P*1̄. The refinement utilized  $w^{-1} = \sigma^2(F_o^2) + (0.1151p)^2 + 251.4963p$ , where  $p = (F_o^2 + 2F_c^2)/3$ . The tungsten atoms were refined anisotropically, but the data quality mandated an isotropic refinement for the remaining heavy atoms. Hydrogens were included at calculated positions. Constraints were applied to the  $^t\text{Bu}_3\text{Si}$  fragments such that chemically equivalent inter- and intraatomic distances utilized the same least-squares variables (i.e., all  $d(\text{Si-C})$  values are equivalent; all  $d(\text{C-C})$  values are equivalent, etc.). A diffusely formed and positionally disordered small molecule was located in an area remote from either compound near the center of symmetry; it was treated and refined as four carbon atoms per asymmetric unit.

3.  $(^t\text{Bu}_3\text{SiN}=\text{C})(^t\text{Bu}_3\text{SiNH})\text{W}(\text{CHCCH}_2)$  (**1-CHCCH<sub>2</sub>**). A colorless block ( $0.2 \times 0.15 \times 0.1$  mm) of **1-CH=C=CH<sub>2</sub>**, obtained by slow evaporation of a hexane solution, was immersed in polyisobutylene, extracted with a glass fiber, and placed under a 173 K nitrogen stream on the goniometer head of a Siemens SMART CCD area detector system equipped with a fine-focus Mo X-ray tube ( $\lambda = 0.71073$  Å). Preliminary diffraction data revealed a monoclinic crystal system, and a hemisphere routine was used for data collection. The data were processed via the Bruker SAINT program to afford 27 007 reflections, 10 355 of which were symmetry independent ( $R_{\text{int}} = 0.0663$ ) and 5347 were greater than  $2\sigma(I)$ . The data were corrected for absorption with SADABS, and the structure was solved by direct methods (SHELXS), completed by difference Fourier syntheses, and refined by full-matrix least-squares procedures (SHELXL).<sup>51</sup> The refinement utilized  $w^{-1} = \sigma^2(F_o^2) + (0.0149p)^2 + 3.287p$ , where  $p = (F_o^2 + 2F_c^2)/3$ . All non-hydrogen atoms were refined anisotropically, and hydrogen atoms were included at calculated positions.

## ■ ASSOCIATED CONTENT

### ■ Supporting Information

CIF files giving crystal data for **1-CH<sub>3</sub>**, **1-<sup>t</sup>PrMe**, and **1-CH=C=CH<sub>2</sub>**. This material is available free of charge via the Internet at <http://pubs.acs.org>.

## ■ AUTHOR INFORMATION

### Corresponding Author

\*Fax: 607 255 4173. E-mail: [ptw2@cornell.edu](mailto:ptw2@cornell.edu).

## ■ ACKNOWLEDGMENTS

P.T.W. thanks the NSF (Nos. CHE-9528914 and CHE-1055505) and Cornell University for financial support.

## ■ REFERENCES

- (1) Bernskoetter, W. H.; Schauer, C. K.; Goldberg, K. I.; Brookhart, M. *Science* **2009**, *326*, 553–556.
- (2) (a) Geftakis, S.; Ball, G. E. *J. Am. Chem. Soc.* **1998**, *120*, 9953–9954. (b) Geftakis, S.; Ball, G. E. *J. Am. Chem. Soc.* **1999**, *121*, 6336–

6336. (c) Young, R. D.; Hill, A. F.; Hillier, W.; Ball, G. E. *J. Am. Chem. Soc.* **2011**, *133*, 13806–13809.

(3) (a) Lawes, D. J.; Darwish, T. A.; Clark, T.; Harper, J. B.; Ball, G. E. *Angew. Chem., Int. Ed.* **2006**, *45*, 4486–4490. (b) Ball, G. E.; Brookes, C. M.; Cowan, A. J.; Darwish, T. A.; George, M. W.; Kawanami, H. K.; Portius, P.; Rourke, J. P. *Proc. Natl. Acad. Sci. U.S.A.* **2007**, *104*, 6927–6932.

(4) (a) Bromberg, S. E.; Yang, H.; Asplund, M. C.; Lian, T.; McNamara, B. K.; Kotz, K. T.; Yeston, J. S.; Wilkens, M.; Frei, H.; Bergman, R. G.; Harris, C. B. *Science* **1997**, *278*, 260–263. (b) Lian, T.; Bromberg, S. E.; Yang, H.; Proulx, G.; Bergman, R. G.; Harris, C. B. *J. Am. Chem. Soc.* **1996**, *118*, 3769–3770. (c) Asplund, M. C.; Snee, P. T.; Yeston, Y. S.; Wilkens, M. J.; Payne, C. K.; Yang, H.; Kotz, K. T.; Frei, H.; Bergman, R. G.; Harris, C. B. *J. Am. Chem. Soc.* **2002**, *124*, 10605–10612.

(5) Sawyer, K. R.; Cahoon, J. F.; Shanoski, J. E.; Glascoe, E. A.; King, M. F.; Schlegel, J. P.; Zoerb, M. C.; Hapke, M.; Hartwig, J. F.; Webster, C. E.; Harris, C. B. *J. Am. Chem. Soc.* **2010**, *132*, 1848–1859.

(6) (a) Calladine, J. A.; Torres, O.; Ansley, M.; Ball, G. E.; Bergman, R. G.; Curley, J.; Buckett, S. B.; George, M. W.; Gilson, A. I.; Lawes, D. J.; Perutz, R. N.; Sun, X. Z.; Vollhardt, K. P. C. *Chem. Sci.* **2010**, *1*, 622–630. (b) Calladine, J. A.; Duckett, S. B.; George, M. W.; Matthews, S. L.; Perutz, R. N.; Torres, O.; Vuong, K. Q. *J. Am. Chem. Soc.* **2011**, *133*, 2303–2310.

(7) Churchill, D. G.; Janak, K. E.; Wittenberg, J. S.; Parkin, G. *J. Am. Chem. Soc.* **2003**, *125*, 1403–1420.

(8) Gould, G. L.; Heinekey, D. M. *J. Am. Chem. Soc.* **1989**, *111*, 5502–5504.

(9) Gross, C. L.; Girolami, G. S. *J. Am. Chem. Soc.* **1998**, *120*, 6605–6606.

(10) Bernskoetter, W. H.; Hanson, S. K.; Buzak, S. K.; Davis, Z.; White, P. S.; Swartz, R.; Goldberg, K. I.; Brookhart, M. *J. Am. Chem. Soc.* **2009**, *131*, 8603–8613.

(11) Jones, W. D. *Acc. Chem. Res.* **2003**, *36*, 140–146.

(12) Evans, D. R.; Drovetskaya, T.; Bau, R.; Reed, C. A.; Boyd, P. D. *W. J. Am. Chem. Soc.* **1997**, *119*, 3633–3634.

(13) Castro-Rodriguez, I.; Nakai, H.; Gantzel, P.; Zakharov, L. N.; Rheingold, A. L.; Meyer, K. *J. Am. Chem. Soc.* **2003**, *125*, 15734–15735.

(14) Wolczanski, P. T. *Chem. Commun.* **2009**, 740–757.

(15) Cundari, T. R.; Klinckman, T. R.; Wolczanski, P. T. *J. Am. Chem. Soc.* **2002**, *124*, 1481–1487.

(16) (a) Cundari, T. R. *J. Am. Chem. Soc.* **1992**, *114*, 10557–10563. (b) Cundari, T. R. *Organometallics* **1993**, *12*, 4971–4978. (c) Cundari, T. R. *Organometallics* **1994**, *13*, 2987–2994.

(17) (a) Benson, M. T.; Cundari, T. R.; Moody, E. W. *J. Organomet. Chem.* **1995**, *504*, 1–13. (b) Cundari, T. R.; Klinckman, T. R. *Inorg. Chem.* **1998**, *37*, 5399–5401. (c) Cundari, T. R.; Matsunaga, N.; Moody, E. W. *J. Phys. Chem.* **1996**, *100*, 6475–6483.

(18) Cundari, T. R.; Pierpont, A. W.; Rabaa, H. *Int. J. Quantum Chem.* **2006**, *106*, 1611–1619.

(19) Bennett, J. L.; Wolczanski, P. T. *J. Am. Chem. Soc.* **1994**, *116*, 2179–2180.

(20) (a) Bennett, J. L.; Wolczanski, P. T. *J. Am. Chem. Soc.* **1997**, *119*, 10696–10719. (b) Bennett, J. L.; Vaid, T. P.; Wolczanski, P. T. *Inorg. Chim. Acta* **1998**, *270*, 414–423.

(21) Slaughter, L. M.; Wolczanski, P. T.; Klinckman, T. R.; Cundari, T. R. *J. Am. Chem. Soc.* **2000**, *122*, 7953–7975.

(22) Cummins, C. C.; Schaller, C. P.; Van Duyne, G. D.; Wolczanski, P. T.; Chan, E. A.-W.; Hoffmann, R. *J. Am. Chem. Soc.* **1991**, *113*, 2985–2994.

(23) (a) Schaller, C. P.; Cummins, C. C.; Wolczanski, P. T. *J. Am. Chem. Soc.* **1996**, *118*, 591–611. (b) Cummins, C. C.; Baxter, S. M.; Wolczanski, P. T. *J. Am. Chem. Soc.* **1988**, *110*, 8731–8733.

(24) Schaller, C. P.; Bonanno, J. B.; Wolczanski, P. T. *J. Am. Chem. Soc.* **1994**, *116*, 4133–4134.

(25) de With, J.; Horton, A. D. *Angew. Chem., Int. Ed. Engl.* **1993**, *32*, 903–905.



- (26) de With, J.; Horton, A. D.; Orpen, A. G. *Organometallics* **1993**, *12*, 1493–1496.
- (27) Schaller, C. P.; Wolczanski, P. T. *Inorg. Chem.* **1993**, *32*, 131–144.
- (28) Schafer, D. F. II; Wolczanski, P. T. *J. Am. Chem. Soc.* **1998**, *120*, 4881–4882.
- (29) Schafer, D. F., II Ph.D. Thesis, Cornell University, 1999.
- (30) Schafer, D. F., II; Wolczanski, P. T.; Lobkovsky, E. B. *Organometallics* **2011**, *30*, DOI: 10.1021/om200597z.
- (31) Lowry, T. H.; Richardson, K. S. *Mechanism and Theory in Organic Chemistry*, 3rd ed.; Harper and Row: New York, 1987.
- (32) Wigley, D. E. *Prog. Inorg. Chem.* **1994**, *42*, 239–482.
- (33) Nugent, W. A.; Mayer, J. M. *Metal-Ligand Multiple Bonds*; Wiley: New York, 1988.
- (34) Carpenter, B. K. *Determination of Reaction Mechanisms*; Wiley-Interscience: New York, 1984.
- (35) (a) Griller, D.; Ingold, K. U. *Acc. Chem. Res.* **1980**, *13*, 317–323. (b) Newcomb, M.; Toy, P. H. *Acc. Chem. Res.* **2000**, *33*, 449–455.
- (36) Bowry, V. W.; Luszyk, J.; Ingold, K. U. *J. Am. Chem. Soc.* **1991**, *113*, 5687–5698.
- (37) (a) Chatgililoglu, C.; Ingold, K. U.; Scaiano, J. C. *J. Am. Chem. Soc.* **1981**, *103*, 7739–7742. (b) Schmid, P.; Griller, D.; Ingold, K. U. *Int. J. Chem. Kinet.* **1979**, *11*, 333–338.
- (38) (a) Hoyt, H. M.; Bergman, R. G. *Angew. Chem., Int. Ed.* **2007**, *46*, 5580–5582. (b) Hoyt, H. M.; Michael, F. E.; Bergman, R. G. *J. Am. Chem. Soc.* **2004**, *126*, 1018–1019. (c) Lee, S. Y.; Bergman, R. G. *J. Am. Chem. Soc.* **1995**, *117*, 5877–5878. (d) Walsh, P. J.; Hollander, F. J.; Bergman, R. G. *J. Am. Chem. Soc.* **1988**, *110*, 8729–8731.
- (39) Jones, W. D. *Inorg. Chem.* **2005**, *44*, 4475–4484.
- (40) Ng, S. H. K.; Adams, C. S.; Hayton, T. W.; Legzdins, P.; Patrick, B. O. *J. Am. Chem. Soc.* **2003**, *125*, 15210–15223.
- (41) (a) Tseng, T. W.; Wu, I. Y.; Tsai, J. H.; Lin, Y. C.; Chen, D. J.; Lee, G. H.; Cheng, M. C.; Wang, Y. *Organometallics* **1994**, *13*, 3963–3971. (b) Keng, R. S.; Lin, Y. C. *Organometallics* **1990**, *9*, 289–291.
- (42) (a) Ang, W. H.; Cordiner, R. L.; Hill, A. F.; Perry, T. L.; Wagler, J. *Organometallics* **2009**, *28*, 5568–5574. (b) Bussetto, L.; Marchetti, F.; Zucchini, S.; Zanotti, V. *Eur. J. Inorg. Chem.* **2005**, 3250–3260. (c) Wells, M. B.; McConathy, J. E.; White, P. S.; Templeton, J. L. *Organometallics* **2002**, *21*, 5007–5020. (d) Chetcuti, M. J.; McDonald, S. R. *Organometallics* **2002**, *21*, 3162–3168. (e) Ogoshi, S.; Nishida, T.; Fukunishi, Y.; Tsutsumi, K.; Kurosawa, H. *J. Organomet. Chem.* **2001**, *620*, 190–193.
- (43) Polse, J. L.; Andersen, R. A.; Bergman, R. G. *J. Am. Chem. Soc.* **1998**, *120*, 13405–13414.
- (44) Rosenfeld, D. C.; Wolczanski, P. T.; Barakat, K. A.; Buda, C.; Cundari, T. R.; Schroeder, F. C.; Lobkovsky, E. B. *Inorg. Chem.* **2007**, *46*, 9715–9735.
- (45) (a) Mayer, J. M. *J. Phys. Chem. Lett.* **2011**, *2*, 1481–1489. (b) Warren, J. T.; Mayer, J. M. *Proc. Natl. Acad. Sci. U.S.A.* **2010**, *107*, 5282–5287.
- (46) Manner, V. W.; Lindsay, A. D.; Mader, E. A.; Harvey, J. N.; Mayer, J. M. *Chem. Sci.* **2011**, in press.
- (47) Collman, J. P.; Hegedus, L. S.; Norton, J. R.; Finke, R. G. *Principles and Applications of Organotransition Metal Chemistry*; University Science Books: Mill Valley, CA, 1987.
- (48) (a) Williams, G. M.; Gell, K. I.; Schwartz, J. *J. Am. Chem. Soc.* **1980**, *102*, 3660–3662. (b) Gell, K. I.; Schwartz, J. *J. Am. Chem. Soc.* **1981**, *103*, 2687–2695.
- (49) (a) Adams, C. S.; Legzdins, P.; Tran, E. *J. Am. Chem. Soc.* **2001**, *123*, 612–624. (b) Adams, C. S.; Legzdins, P.; McNeil, W. S. *Organometallics* **2001**, *20*, 4939–4955. (c) Adams, C. S.; Legzdins, P.; Tran, E. *Organometallics* **2002**, *21*, 1474–1486.
- (50) States, D. J.; Haberkorn, R. A.; Ruben, D. J. *J. Magn. Reson.* **1982**, *48*, 286–289.
- (51) Sheldrick, G. M. *SHELXTL: An Integrated System for Solving, Refining and Displaying Crystal Structures from Diffraction Data*; University of Gottingen, Gottingen, Germany, 1981.